Landscape and Urban Planning 195 (2020) 103709

Contents lists available at ScienceDirect

Landscape and Urban Planning

journal homepage: www.elsevier.com/locate/landurbplan

# Urban mapping needs up-to-date approaches to provide diverse perspectives of current urbanization: A novel attempt to map urban areas with nighttime light data

Xiaofang Hu[a,b], Yuguo Qian[a,b], Steward T.A. Pickett[c], Weiqi Zhou[a,b,*]

[a] State Key Laboratory of Urban and Regional Ecology, Research Center for Eco-Environmental Sciences, Chinese Academy of Sciences, Beijing 100085, China
[b] University of Chinese Academy of Sciences, Beijing 100049, China
[c] Cary Institute of Ecosystem Studies, Millbrook, NY 12545, United States

ARTICLE INFO

*Keywords:*
Urban mapping
Perspectives of urban
Nighttime light
DMSP/OLS
Urban fringe

ABSTRACT

Quantifying the spatial and temporal changes of urban extent is important for understanding the burgeoning process of urbanization. Numerous well-performing methods have been used to map urban areas and detect urban changes using nighttime light data, but many of these methods assume that the urban area is equivalent to regions with high percentages of impervious surfaces or developed land. We present an approach to efficiently map urban areas at the regional scale, which also provides opportunities to recognize urban extents from different theoretical perspectives. In our approach, appropriate demarcating criteria and urban indicators were chosen based on understanding the current state of urbanization of the study area. After object-based segmentation and detection of initial urban centers, urban patches are discerned by expanding from these initial urban centers through a grouping algorithm, delineating the relative fringes of the urban area. We tested this new approach for mainland China, using 2010 Defense Meteorological Satellite Program/Operational Linescan System nighttime light data and county-level administrative units. We found a total urban area of 146,806 $km^2$, spread across 2489 counties and amounting to 1.5% of the land in mainland China. The delineated boundary of the urban patches had different values by compass direction. Mean values of fringes and sizes of different urban patches varied greatly across regions. We detected all provincial capitals, 97.3% of the prefecture-level cities and 91.0% of the county-level cities. This approach is thus capable of identifying urban patches with reliable accuracy at the regional scale.

## 1. Introduction

Mapping where urban growth occurs can help us understand current dynamics of urbanization and its social-ecological causes and consequences (Grimm et al., 2008; Pickett & Zhou, 2015). Urban mapping contributes to a broad range of studies, such as urban sprawl, comparative studies of biodiversity, and regional planning and management (Aronson et al., 2014; Zhou, Li, Asrar, Smith, & Imhoff, 2018). Although such mapping is necessary in order to define urban study areas or to conduct analysis, there is no universally accepted definition of the urban, nor is there a distinct separating line between the urban and non-urban areas in the real world (Brenner & Schmid, 2014; McIntyre, Knowles-Yanez, & Hope, 2000).

One potential solution for improving urban mapping would be to recognize relatively urban areas according to specific urban characteristics. Regions with dense buildings could be regarded as urban areas, so do other physical or functional structures such as lighting systems, drainage systems, and transportation systems from a land-use perspective (Martinuzzi, Gould, & Gonzalez, 2007). These components or structures could all be used to delimit urban areas. Furthermore, "invisible" social or economic urban functions and human perceptions should also be understood as different aspects of the urban fabric (Gandy, 2012; Lefebvre, 2003; Monte-Mór, 2005).

Diverse datasets that represent various aspects of the urban could be used for urban mapping from different perspectives. Land cover datasets are often used to map urban areas, because they represent the direct visual results of human constructions. Nighttime light data are widely used for urban mapping as well, because these data have global coverage and represent the spatial extent of intensively used settlements (Bennett & Smith, 2017; Elvidge et al., 2001; Ma et al., 2015;

* Corresponding author at: State Key Laboratory of Urban and Regional Ecology, Research Center for Eco-Environmental Sciences, Chinese Academy of Sciences, Beijing 100085, China.
*E-mail addresses:* ygqian@rcees.ac.cn (Y. Qian), picketts@caryinstitute.org (S.T.A. Pickett), wzhou@rcees.ac.cn (W. Zhou).

https://doi.org/10.1016/j.landurbplan.2019.103709
Received 1 July 2019; Received in revised form 5 November 2019; Accepted 10 November 2019
Available online 21 November 2019
0169-2046/ 

Zhao et al., 2019). Nighttime light data have advantages in studying urban dynamics at large spatial scales or high temporal frequencies (Small, Pozzi, & Elvidge, 2005; Zhou et al., 2015).

There are two available series of nighttime light data: one is from the Defense Meteorological Satellite Program – Operational Linescan System (DMSP-OLS data), and the other is from the Visible Infrared Imaging Radiometer Suite day-night band carried by the Suomi National Polar-orbiting Partnership (VIIRS data). DMSP-OLS data have a lower resolution of 30 arc second (about 1 km), but a longer time series released from 1992 to 2013. The nighttime stable light composites have been used most widely in research studies, because the effects from clouds, fires, and aurora have been largely removed from these images (Zhao et al., 2019). The blooming effects (which can cause dark regions to be bright in the images due to light reflections or coarse resolutions), oversaturation, and lack of calibration among years are major problems of DMSP-OLS data (Bennett & Smith, 2017; Elvidge, Sutton, Tuttle, Ghosh, & Baugh, 2009; Yi, Zeng, & Wu, 2016; Zhao et al., 2019). The VIIRS dataset is an advanced version of nighttime light data initiated in April 2012 that has a higher spatial resolution of 15 arc second (about 500 m). This dataset provides monthly-average composite images that have on-board calibrations, yielding reduced blooming and saturation effects (Bennett & Smith, 2017; Elvidge, Baugh, Zhizhin, Hsu, 2013; Elvidge, Zhizhin, Hsu, & Baugh, 2013). However, the satellite passes given points at around 01:30 locally, when there is likely to be less human activity (Bennett & Smith, 2017; Elvidge, Baugh et al., 2013; Elvidge, Zhizhin et al., 2013). The failure to capture LED lights that emit at wavelengths below 500 nm also makes it less used for urban detection (Bennett & Smith, 2017).

Most previous studies use the long-term DMSP-OLS data to map urban areas, and the thresholding approaches have long been the foci of these mapping studies because of the blooming effects (Henderson, Yeh, Gong, Elvidge, & Baugh, 2003; Imhoff, Lawrence, Stutzer, & Elvidge, 1997; Liu, He, Zhang, Huang, & Yang, 2012; Tan, 2016; Zhou et al., 2014). The blooming effects of the data would make regions without light be seen as bright places in the satellite images. Using certain values of the brightness as thresholds to mitigate the blooming effects is a type of approach to map urban areas (Zhao et al., 2019). Current thresholding approaches used to detect urban fringes can be categorized into two types. The first typically uses a fixed empirical threshold for the whole country or region to identify urban areas (Henderson et al., 2003; Imhoff et al., 1997; Liu et al., 2012). This approach assumes cities in a given region have similar features, so that the same threshold can be applied to all the cities in that same region. However, cities may have different values of brightness even if they are close to each other or have similar physical sizes.

The second approach calculates optimal thresholds for different cities based on relationships between the night light data and ancillary data. This type of analysis can be more accurate but is more complicated to conduct. For example, the Overglow Removal Model (ORM) relies on atmospheric conditions, topography, elevation, and regional lighting techniques to determine thresholds, which could be very accurate if all the relevant data are available (Bennett & Smith, 2017; Townsend & Bruce, 2010). Moreover, applications of this approach identify thresholds based on relationships and parameters calculated through high resolution land-cover data (Cao, Chen, Imura, & Higashi, 2009; Cheng et al., 2016; Lu, Tian, Zhou, & Ge, 2008; Tan, 2016; Xie & Weng, 2016; Yang, He, Zhang, Han, & Du, 2013; Zhou et al., 2015, 2014). These relationships and parameters change across regions and vary by time, which requires a large amount of work on the land cover classification from high resolution images (Li & Zhou, 2017; Xie & Weng, 2016).

In addition to the methodological problems identified above, few thresholding efforts discuss what they are mapping and what reference they are using when they provide new mapping methods. Some studies did not realize the necessity to define urban areas, but more often took the assumption for granted that urban areas were equivalent to impervious surfaces or the developed land (Chen et al., 2019). Therefore mapping results based on land cover data have often been used as the reference to validate urban extents derived from the nighttime light data (Cheng et al., 2016; Huang, Schneider, & Friedl, 2016; Yi et al., 2016; Zhao et al., 2019; Zhou et al., 2014). Based on the perspectives and assumptions about urban areas reviewed above, most studies have aimed to develop a universal method that could be applied everywhere in the world. However, recent urban theories suggest that we should recognize the contemporary urban world as complex mosaics or processes, and the scope of the urban should not be decided only by the visual physical structures (Brenner & Schmid, 2014; Grove, Cadenasso, Pickett, Burch, & Machlis, 2015).

Rapid and extensive urban spread as well as the current understanding of urbanization require up-to-date, comparable, and efficient urban mapping approaches. Improvements in nighttime light data and the emergence of location-tagged data also demand updates for an efficient approach that can be used to demarcate urban areas based on diverse datasets (Klotz, Kemper, Geiß, Esch, & Taubenböck, 2016; Xie & Weng, 2016; Zhao et al., 2019). In this paper, we present a new approach that integrates object-based image analysis with a grouping algorithm to automatically and efficiently map urban areas at the regional scale. Rather than using a fixed threshold, this approach sets up relative boundaries for different urban patches by taking local contexts into consideration. We test this new approach for mainland China, using the 2010 nighttime light data from the Defense Meteorological Satellite Program/Operational Linescan System and the officially designated county-level administrative units.

## 2. Study area

We selected China as the experimental area to test our method, because on the one hand it has complicated topography (Fig. 1) and possesses cities of different sizes and diverse functions experiencing different levels of urbanization (Cheng et al., 2016). On the other hand, although cities in China vary by region and development status, the basic ideas of city construction and management remain the same.

Cities in East and South China are more developed and tend to grow in continuous clusters as urban agglomerations. Cities in the west and north are less developed. In these regions, several big cities play the roles of “engines” for the area, and the others are smaller and scattered. The unbalanced development of cities can also be illustrated by the sizes of counties (Fig. 1). Administrative counties in better developed regions have smaller areas because of their higher density of population and resources.

Cities and towns in China are administered under powers from several levels of government – provincial, prefecture- and county-levels (Table 1; Box 1). The county is the smallest unit that can delimit a city or part of a city. These divided administrative units are adjusted by the government as an area urbanizes, so they change every now and then. The county-level units change more rapidly compared to the provincial or prefecture-level units. For instance, there were 2861, 2856, and 2851 county-level administrative units in the years of 2000, 2010, and 2016 respectively (Wu & Ding, 2018).

Because the terms used to designate different administrative levels of Chinese urbanization might be unfamiliar to many readers, we clarify the meaning of urban labels we used in this paper as below (Table 1; Box 1).

**BOX 1**

: Terms for administrative units & cities in China.

In China, places are named and administratively bordered on maps as “SHENG”, “SHI”, ‘XIAN‘/ ‘’QU”, “JIE DAO”/”XIANG”/ ”ZHEN”.

Under the administrative division, SHENG means province, the first-level administrative unit. SHI is the prefecture-level

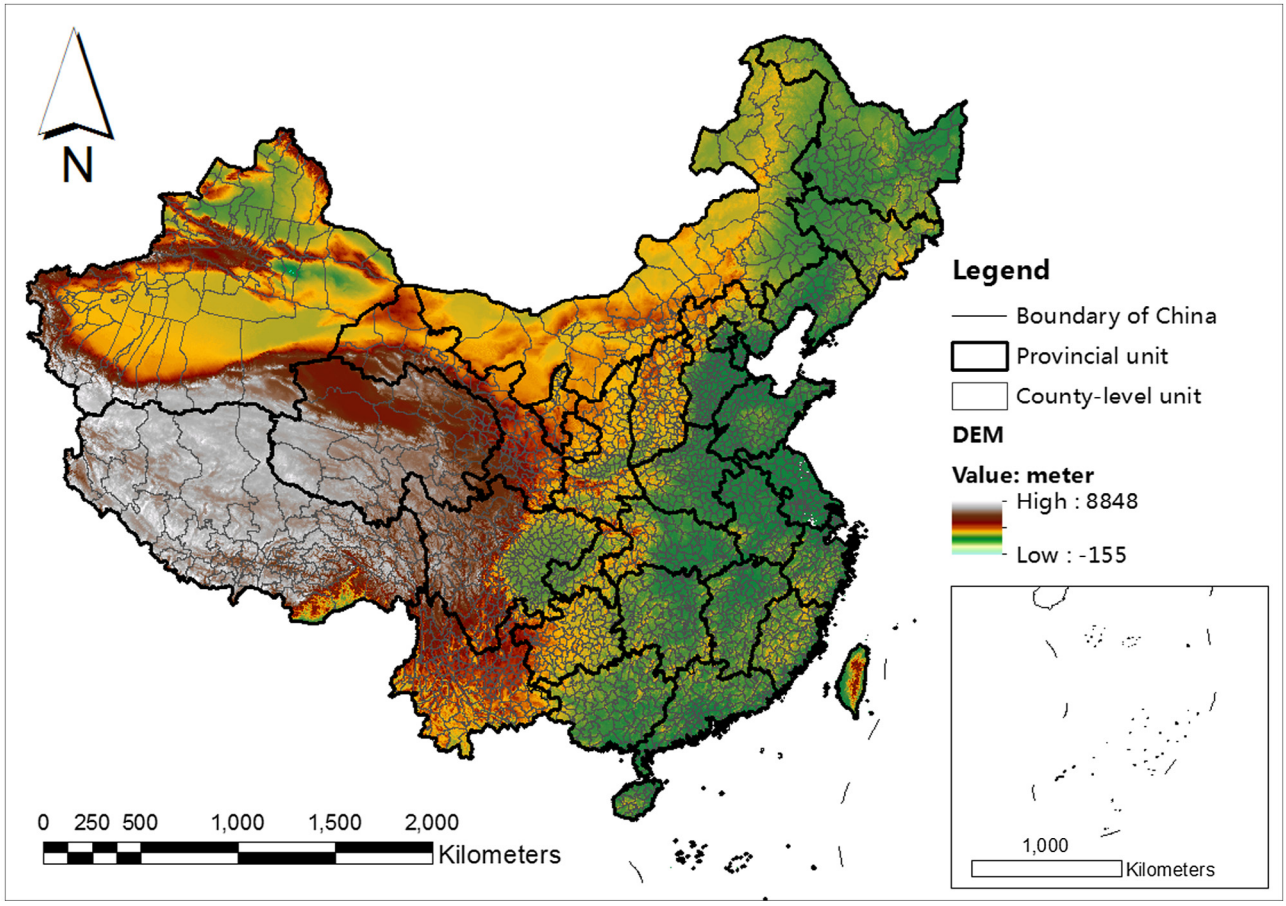


**Fig. 1.** Provincial, county-level administrative units and topography of China. The black lines are provincial boundaries while the grey lines are county-level boundaries. The color from snow white to light green represents changes in altitude. The highest point is in the Himalayas with an altitude of 8848 m. The lowest point is in Xinjiang with an altitude of −155 m. (For interpretation of the references to color in this figure legend, the reader is referred to the web version of this article.)

division under SHENG and consists of XIAN/QU. XIAN/QU means county. JIE DAO/XIANG/ZHEN is the fourth-level administrative unit under XIAN/QU, which has little power and seems to be declining. More money assigned by government goes to higher-level units.

SHI, in addition to the administrative meaning of prefectures under provincial units, also refers to "city" - municipality, provincial-, prefecture- or county-level cities. Municipalities are "level-up" cities from prefecture-level cities, meaning they have the same power level as provinces. Beijing, Tianjin, Shanghai and Chongqing are the only four municipalities currently. A provincial city is a special type of prefecture-level city that also functions as the capital of the province. Municipalities are generally bigger than prefecture-level cities, as they receive more funding from the central finances. Prefecture-level cities are generally bigger than county-level cities, as prefectures have been assigned power to administer their counties, from which they can accumulate resources and land. Prefecture-level cities might consist of several county-level cities or towns.

XIAN and QU are administered by SHI, but they are different. XIAN is usually far from its host SHI and could have an urban patch inside as a county-level city/town. QU is close to its host SHI and is more likely to have an urban patch as part of a municipality or prefecture-level city.

JIE DAO, XIANG and ZHEN act as postal units rather than administrative units nowadays in China. They are units using an idea that is similar to watershed. They can be a region that has one main street in the middle (like the main stream) and linked with several smaller streets (like tributaries). In a city, they are called JIE DAO. In rural regions, bigger units are called ZHEN while smaller units are called XIANG.

## 3. Datasets

### 3.1. Nighttime light data

We used the stable lights of the DMSP-OLS as the major data to test our approach. The DMSP-OLS dataset provides an image of stable lights each year from 1992 to 2013. Each image of stable lights is made of all available cloud-free DMSP-OLS data for the specific calendar year. The data of stable lights record nightlights through DN values from 0 to 63. The value "0" means dark and "63" is the maximum brightness. The stable lights from 2010 to 2013 were obtained from the NOAA website (http://ngdc.noaa.gov/eog/dmsp). The data of 2010 were used to map the urban areas, while the data of 2011, 2012 and 2013 were used to filter the inconsistent lights that disappeared in later years.

The DMSP-OLS satellite passes at around 20:30–21:30 locally, which is more representative for human activities than the VIIRS data consisting of nightlight at 01:30. Nightlights captured earlier, at around 21:00 are likely to include light from residential, commercial and fundamental street light sources. Nightlights measured at 01:30 might not include some of the sources above based on different lifestyles in different regions. Further militating against the use of VIIRS for extracting urban areas (Shi et al., 2014) is the lack of methods for filtering out fires and aurora (Bennett & Smith, 2017). Consequently, we chose the DMSP-OLS data for our analyses

**Table 1**
Definitions of terms used in the paper.

Defined specifically in this paper

| Term | Meaning | Visual or descriptive examples |
|---|---|---|
| The urban/urban areas/ urban regions | Human settlements and functionally-related regions that have relatively more street lamps, automobile movements, residential and commercial regions that have lights at night. We assume nightlife is a type of urban lifestyle in contemporary China. | Seen from nighttime light maps, relatively brighter areas than their surrounding regions. Fig. 4. |
| Urban patch | Delineated urban areas based on the definition of the urban above. | Mapped results in Fig. 5. |
| *Urban center* | Urban patches that have high density of roads, buildings, shops and restaurants that attract people and generate nightlife. | Seen from nighttime light maps, urban patches that have the highest values of brightness inside counties or extreme high values at the country scale. |
| *City/town* | Urban patches that have bigger or smaller sizes. Big patches are cities, and small patches are towns. The way we use these terms in the paper is different from the administratively divided city or town. | Figs. 5, 7, 8 |
| *County-level city/town* | Urban patches inside counties, the basic unit of urban patches. | Xinzheng city in Zhengzhou Prefecture, Henan Province. We take black dots in Fig. 2 as reference. |
| *Prefecture-level city* | Urban patches, connected county-level cities/towns inside prefectures. | Wuxi city in Wuxi Prefecture, Jiangsu Province. We take green dots in Fig. 2 as reference. |
| *Provincial capital* | Urban patches, a special type of prefecture-level city that functions as the capital city of a province or a municipality. | Zhengzhou city in Zhengzhou Prefecture, which is also the provincial capital of Henan Province. We take yellow dots in Fig. 2 as reference. |

Defined and divided administratively by the government

| Term | **Meaning** | **Visual or descriptive examples** |
|---|---|---|
| Province/provincial unit | Consists of urban and non-urban patches. Covered all areas as the provincial division of the country. The highest level of administration under the national government control. | Henan, Jiangsu, Guangdong Provinces. Divided by the thick black provincial boundaries in Fig. 1. |
| Municipality | Consists of urban and non-urban patches. Special prefectures that have the same administrative level of provinces. | Beijing, Tianjin, Shanghai, and Chongqing Municipalities, divided by thick black provincial boundaries in Fig. 1. |
| Prefecture/prefecture-level unit | Consists of urban and non-urban patches. Covered all areas as the prefecture-level division of the country, and the power level of which is under the province. | Grey units in Fig. 2. |
| County/county-level unit | Consists of urban and non-urban patches. Covered all areas as county-level division of the country, and the power level of which is under the prefecture. | Counties are divided by grey county-level boundaries in Fig. 1. |

### *3.2. Administrative units and other data for accuracy assessment*

The county-level administrative units of China were used as the ancillary data to detect urban areas (Fig. 1). There are 2811 county-level units covering mainland China (except for Hong Kong, Macao, Taiwan and islands on the South Sea), according to the data obtained from the National Geomatics Center of China (NGCC; http://ngcc.sbsm.gov.cn). There is a slight discrepancy in the NGCC data since there were 2856 county-level units in 2010 except for Hong Kong, Macao and Taiwan according to government files about administrative zones (Wu & Ding, 2018).

Locations of cities, urban boundary dataset, and the land cover of China were used as the reference against which to evaluate the performance of our method (Fig. 2). The geographic locations of cities that exist at different administrative levels in China, were obtained from Baidu Maps. There are 31 provincial capitals, 332 prefecture-level cities (excluding Sansha in South China Sea) and 2880 county-level cities/towns in mainland China (circles and triangles in Fig. 2). Those black triangles for county-level cities/towns are urban regions inside county-level units, such as for Haidian and Chaoyang, which are counties inside Beijing municipality.

The points locating cities and towns from Baidu Maps are not the physical centers of those urban areas. In fact, except for huge cities such as Beijing and Shanghai, most of these dots are located at the urban constructed fringes. The dots in the map (Fig. 2) are not overlapped when a city represents different administrative levels. For instance, except for Beijing, Tianjin, Shanghai and Chongqing, the other 27 provincial capitals are also prefecture-level cities, and there are another 27 dots representing the same prefecture-level cities with green dots, but these locations are different from those yellow dots representing provincial capitals.

The urban boundary dataset contains urban boundaries of 29 cities in China (Fig. 2; Table 2), which was made based on the land cover in 2010 with the resolution of 30 m derived from Landsat satellite. To make this boundary dataset, grids with different sizes were used to delineate urban areas based on the land cover data, and urban areas were defined as connected grid cells in which the proportion of developed land was above 50%.

The 2010 land cover of China at a resolution of 90 m was acquired from the National Ecological and Environmental Assessment Program (2000–2010) and contained the six land-cover classes of forest land, grassland, wetland, cultivated land, developed land, and barren (Ouyang et al., 2016).

## 4. Methodology

We use the idea of “relatively urban” to recognize urban areas. As mentioned in the introduction, urban systems are complex and multi-dimensional, so that there can be different ways to understand and map relatively urbanized regions. Specifically, the urban areas we are demarcating in this paper represent regions that have urban night lives. We assume urban areas in China are likely to have more street lamps, automobile lights and dense residential, commercial and social regions that are brighter at night, so that the night life represents a current urban lifestyle in China (Table 1). Under such a perspective, urban areas could be recognized as clusters of brighter objects than their surrounding areas in the nighttime light maps.

We used county-level units to delineate urban areas using an object-based method. According to the knowledge of how urban areas are administratively organized in China (Fan, Li, & Zhang, 2012; Table 1; Box 1), we found that the county-level boundaries to be useful for finding urban nightlife centers. Since urban areas consist of irregularly-shaped patches, an object-based approach that works on objects is more efficient and suitable than a pixel-based method (Myint, Gober, Brazel,

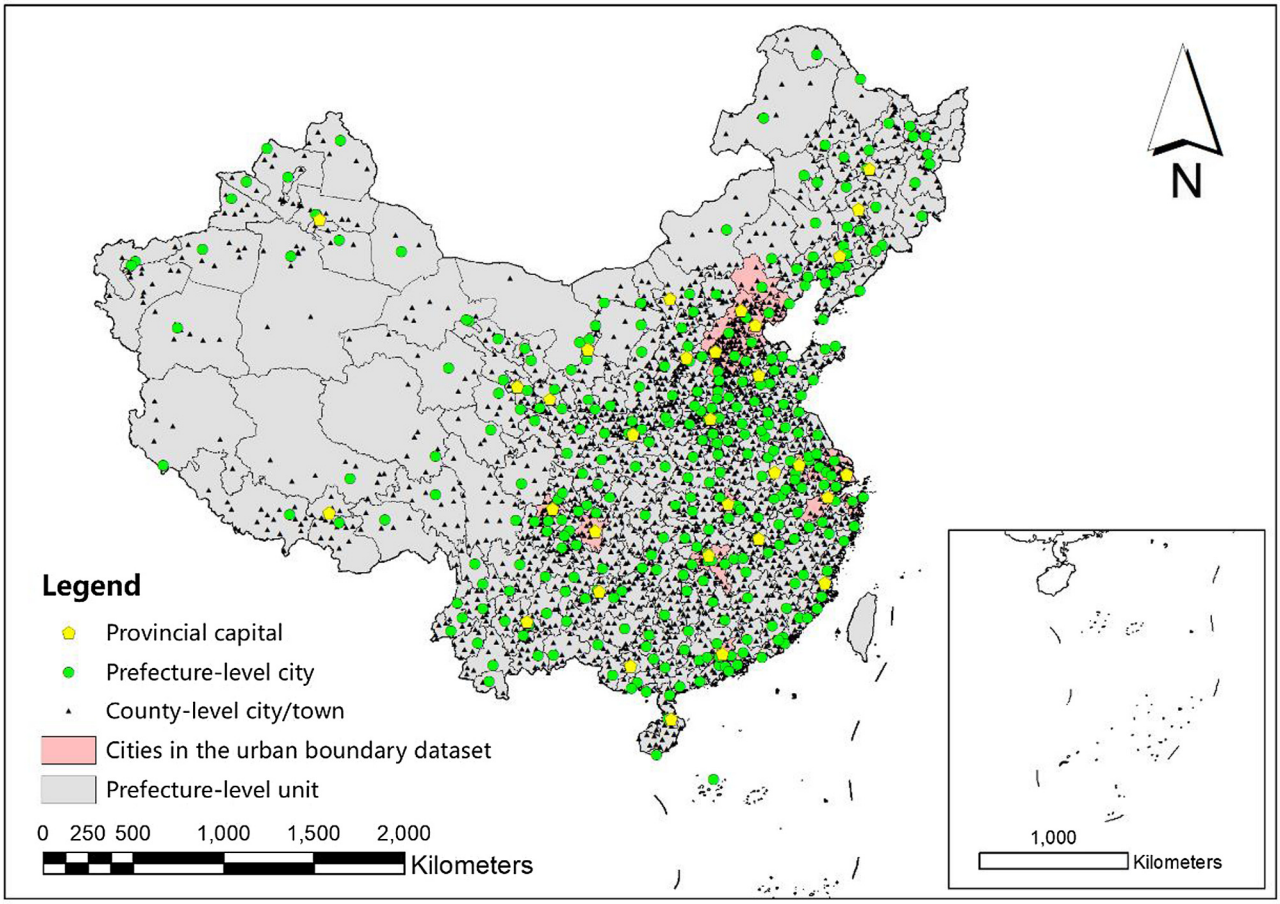


**Fig. 2.** Locations of provincial capitals, prefecture-level cities and county-level cities/towns from Baidu Maps. Cities in the urban boundary dataset are distributed inside the pink units. Grey patches are prefectures. (For interpretation of the references to color in this figure legend, the reader is referred to the web version of this article.)

**Table 2**
Cities in the urban boundary dataset.

| Region | City |
|---|---|
| North | Beijing, Tianjin, Shijiazhuang, Tangshan, Baoding, Cangzhou, Chengde, Hengshui, Langfang, Qinhuangdao, Xingtai |
| Central | Wuhan, Changsha, Xiangtan, Zhuzhou |
| East | Shanghai, Nanjing, Hangzhou, Suzhou, Wuxi, Changzhou, Nantong, Ningbo |
| South | Shenzhen, Guangzhou, Foshan, Dongguan, |
| South-west | Chongqing, Chengdu |

Grossman-Clarke, & Weng, 2011; Zhang, Xiao, Feng, & Yuan, 2017; Zhou, Troy, & Grove, 2008).

Our method includes five steps: 1) preprocessing, 2) object-based segmentation, 3) detection of urban centers, 4) detection of urban fringes, 5) merging, infill, and refinement (Fig. 3). Briefly, we first filtered nighttime light data by removing light pixels that disappeared in later years and ran image segmentation on the filtered image to generate objects. We then identified objects as urban centers based on their brightness. These urban centers then aggregate into larger urban areas based on an optimal grouping algorithm. Finally, we merged and refined the map. We will detail these five steps below. In addition, we also performed an accuracy assessment.

### 4.1. Preprocessing

Through comparing nighttime light data and remote sensing images from 2010 to 2013, we found groups of lit spots in desert and in other non-urban regions, which completely disappeared in later years. According to assumptions that most urban patches in China are currently not expected to shrink (Liu et al., 2012), we filtered the target nighttime light map in 2010 by darkening the light pixels that disappeared in later years. However, in other regions of the world, the filtering methods should be optimized according to local conditions.

We first reclassified the nighttime light images of 2011–2013 to light ("1") and dark ("0") pixels individually, and then overlaid them to create a stable light mask (Liu et al., 2012). Finally, we applied this mask on 2010 data to filter out unstable light pixels. This procedure worked well for removing non-urban lights in China.

### 4.2. Object-based segmentation

We used a multiresolution segmentation algorithm in eCognition© to segment the filtered nighttime light image into objects. This segmentation method can minimize the local heterogeneity of pixels inside the image object and maximize the heterogeneity among objects for a given resolution (Trimble Germany GmbH, 2014). Segmentation is exemplified by the Beijing-Tianjin-Tangshan megaregion (Fig. 4).

We used empirical parameters of shape = 0.1 and color = 0.9, because color (i.e., spectral information, as digital number/DN values in nighttime light data) is the most important information the light data provide. The shape defines the textural homogeneity of objects, which consists of smoothness (0.5) and compactness (0.5). These empirical parameters are commonly-used and well-supported in urban studies (Mathieu, Aryal, & Chong, 2007; Pu, Landry, & Yu, 2011). We did the

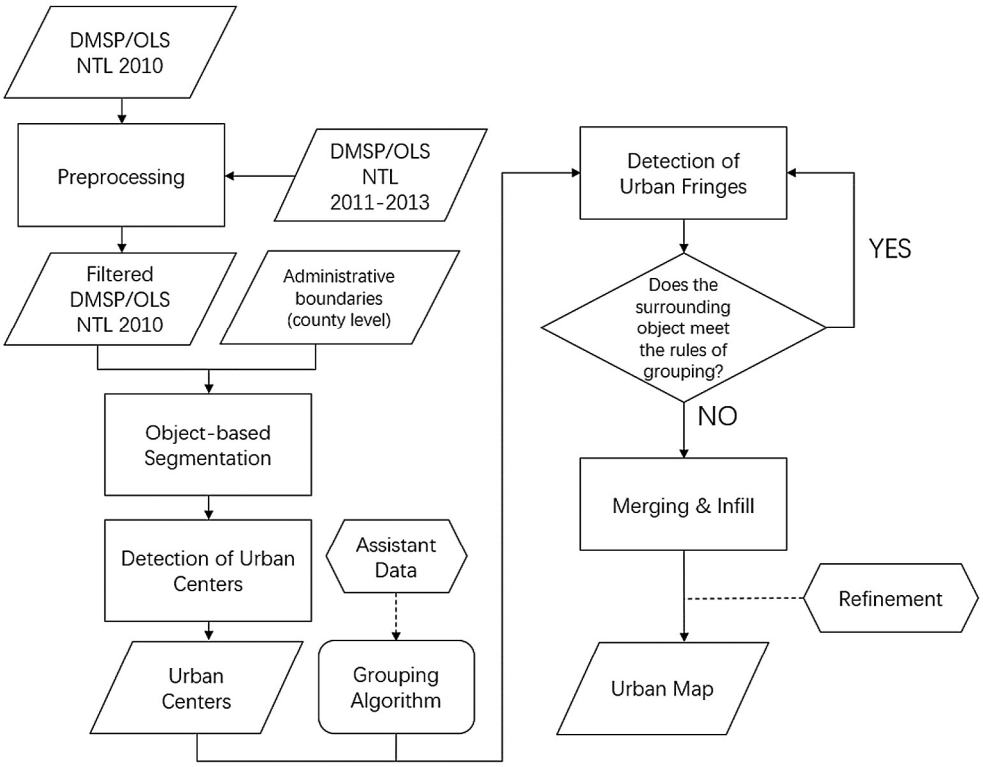


**Fig. 3.** Flowchart of the processing steps.

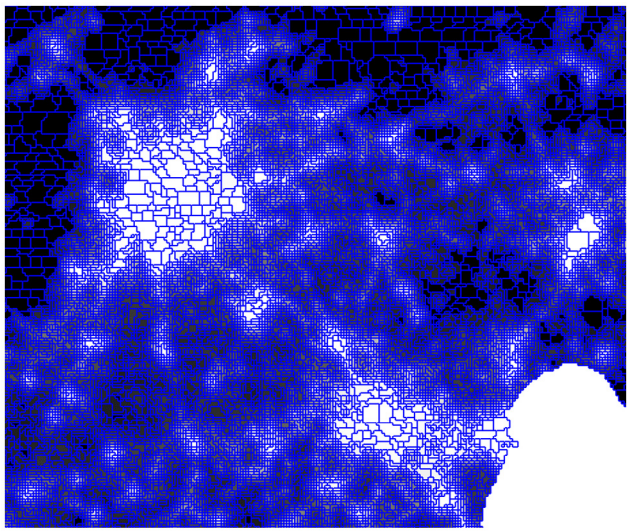

**Fig. 4.** Image segmentation of the Beijing-Tianjin-Tangshan megaregion in.eCognition©.

segmentation at the scale of 1 with previous empirical parameters, so as to make sure that every segmented object has the same DN value and the objects are as fine as possible (Fig. 4). We recommend to do the segmentation at the scale of 1 for DMSP-OLS data, because the DMSP-OLS data have a coarse resolution of 1 km, so that increasing the scale of segmentation would cause the urban mapping to be even coarser and inaccurate. Increasing the scale of segmentation has little influence on urban regions that have been delineated at the scale of 1, but would extract more roads or bright non-urban patches as urban areas. For other high resolution dataset, the scale could be altered to improve the mapping efficiency.

### 4.3. Detection of urban centers

We recognized the brightest objects inside each county as urban centers (Table 1) based on our understandings of the urbanization in China. We found some counties in west China only had scattered villages, and there were no objects with brightness greater than "0". Therefore, to qualify as urban centers, the value of the brightest object must be greater than "0". If there is additional information based on some types of classification suggesting that the brightness of qualified urban centers in China should be above a certain value, then the results of urban centers could be adjusted.

Meanwhile, although there should be only one urban patch inside every county-level unit "officially" according to the management of cities in current China, we are not sure if there are other patches in well-developed counties that would qualify to be urban regions under our definition (Table 1). In addition, the administrative data of county-level units we are using have fewer units than what they should have in 2010 (Section 3.2), which might cause failure to detect enough urban centers. Under such circumstances, we also identified objects that were brighter than 99.5% of all the segmented objects globally as urban centers to avoid losing qualified urban patches in more developed regions. This percentage of 99.5% is an extreme threshold used to make sure that we will not lose patches that are brighter than most of the objects at the country level, even if they might not be recognized as urban regions officially inside some county-level units. The extreme DN value for our 2010 DMSP-OLS data is 58. This method of detection can be applied in regions where the urbanization varies greatly.

### 4.4. Detection of urban fringes

We developed a grouping algorithm for the detection of urban fringes. With this algorithm, the initial urban centers continued "sprawling", that is, merging with surrounding objects, when these surrounding objects were brighter than their neighboring objects. As a result, the initial urban centers and objects that merged with urban

centers were classified as urban areas, and the values of urban fringes were thresholds. We used the loosest condition that any difference would make the urban growth continue. A stricter rule might provide better results, which needs further local investigations to acquire a commonly-accepted reference in advance.

"Brighter than their neighboring objects" means the target object next to the urban center patch has a larger brightness value than the mean value of its surrounding objects, which include the urban center patch and objects that have not yet been classified. To calculate the mean value of the brightness of the surrounding objects, the lengths of borders between the target object and its surroundings were used for weighting. When the urban center has been merged with some surrounding objects, the new patch became slightly darker than before. The urban center would stop merging with other objects when the new object did not meet the criteria of merging, meaning that the new object was statistically too dark to be classified into the same group of objects similar to urban centers inside the same county. We ran the algorithm on all urban centers, and thereby detected urban fringes by extracting urban areas in each county.

With the grouping algorithm, the thresholds of the urban fringe could vary by direction, as a city could have different types of structures at the fringe. This is different from many previous studies that typically used a fixed threshold to identify urban fringes in all directions for a city (He et al., 2006; Imhoff et al., 1997; Liu et al., 2012; Shi et al., 2014; Sutton, 2003). We did not set up stopping boundaries for the spread, so that urban areas could cross administrative boundaries and connect with one another. This allowed us to acquire information on evolving connections among cities. This flexible approach differs from previous studies that set up potential urban areas *a priori* (Zhou et al., 2014, 2015).

Assistant data can provide more information about urban areas in specific studies, and could be used to improve the grouping algorithm. For example, in our study, we did not set up an additional ending criterion, but if we have the data on distributions of some types of night activities, we might be able to use such distributions as reference to promote grouping accuracy.

### 4.5. Merging, infill, and refinement

We first classified all the objects that were entirely enclosed by mapped urban patches as urban objects. We did this because we assume that dark objects (e.g., rivers, lakes, green infrastructures, and other daily functional regions) within cities function together with those bright patches during the day and are important parts of urban areas (Cadenasso, Pickett, & Schwarz, 2007; Grove et al., 2015; Rademacher, Cadenasso, & Pickett, 2019). Therefore, we did not exclude them using NDVI or other metrics as previous studies did (Cao et al., 2009; Cheng et al., 2016; Lu et al., 2008; Xie & Weng, 2016; Yang et al., 2013).

We then merged all the urban patches, and deleted objects that were smaller than 8 $km^2$, which is the size assumed to be too small to function as a city in China (Yang et al., 2013). This particular size is a local refining procedure that could be modified in other regions. In this step, other available and reliable datasets can also be used to refine the results according to the research or management aims, for example to use the Landscan population dataset or cellular signal dataset to delineate urban areas with larger populations.

### 4.6. Accuracy assessment

Currently, the most popular way of conducting the accuracy assessment is to compare the delineated urban areas with those derived from high resolution remote sensing data. Relationships of areas, thresholds, and sometimes a confusion matrix are provided (Xie & Weng, 2016; Zhou et al., 2014). Studies employing such assessments possess different conceptual views of urban mapping from ours. These studies regard discrete and bounded patches having a high percentage of impervious surface as urban areas; therefore, they match nighttime light data to remote sensing images as the way of conducting urban mapping, which necessarily makes their results close to references derived from remote sensing images. Some studies have discussed the possibility that the delimitation of urban systems using nighttime light data might differ from delimitation based on high resolution images (Zou et al., 2017), and that nighttime light maps provide different urban patterns from land cover maps (Uchiyama & Mori, 2017). Some urban mapping studies did not conduct such accuracy assessment (Ginzarly, Roders, & Teller, 2018; Peng, Hu, Liu, Ma, & Zhao, 2018).

However, there are no other commonly-used reference maps, and the accuracy assessment is often required for urban mapping studies. In addition to providing visual mapping results with land cover maps, we compared urban extents with the total area of the developed land inside urban patches at the county level, and with urban areas derived from the urban boundary dataset (Fig. 2; Table 2), to show the results from different perspectives of urban mapping. We also used the locations of provincial capitals, prefecture-level and county-level cities/towns from Baidu Maps to evaluate our urban detection to those administrative realities (Fig. 2). We further compared our results with the modified DMSP-OLS data in which the blooming and saturation effects have been largely removed through a self-adjusting model (the SEAM model from Cao et al., 2019), to evaluate if our mapping approach is influenced by the blooming and saturation effects.

## 5. Results

We delineated 2323 connected urban patches across the mainland of China (Fig. 5). Among all the 2811 administrative counties, urban areas existed in 2489 counties and covered 146,806 $km^2$, that is 1.5% of the mainland China. Some urban areas overspread their county-level boundaries, and some even stretched across prefectures to form regional urban agglomerations. Nearly all provinces had large cities, and in most cases the largest patch was the capital city of the province (Fig. 5).

### 5.1. Thresholds of brightness in the urban fringe

The mean thresholds of urban patches at the prefecture level ranged from 5 to 62 in DN value (Fig. 6). Most of the mean thresholds were between 30 and 50 of the DN values. Spatially, the mean thresholds showed a hierarchical pattern of urban patches in China (Fig. 7). Coastal urban patches tended to have mean thresholds higher than 50. Higher thresholds in other regions turned out to be capital cities and the cities around them, and the brightness of those cities ranged from 40 to 55. Other remote urban patches had lower mean thresholds.

Based on our method, the thresholds for identifying urban areas differed by compass direction for a specific urban patch (Fig. 8). The different values of thresholds suggested that various structures or functions existed in the fringes of a city. Thresholds of the edges also showed connections among different cities in megaregions. For example, in the Yangtze River Delta megaregion, Shanghai city had stronger connections with Suzhou and Wuxi, while Wuxi city had weaker connections with Changzhou city (Fig. 8, C).

Thresholds of urban patches varied by patch size and differed by region. Thresholds were larger for large patches and smaller for small ones (Figs. 7 and 8). Even in Xizang or Xinjiang province, where the economy was below the average among provinces, the thresholds of large patches were around 50. Small patches had much lower thresholds which were lower than 20, and most of those were county-level cities. The thresholds were generally bigger in the eastern and southern parts of China. For example, small urban patches in the Beijing-Tianjin-Hebei megaregion, the Yangtze River Delta megaregion, and the Pearl River Delta megaregion had thresholds higher than 40, much higher than those of urban patches with similar sizes in the southwest of China, such as urban patches in Yunnan, Sichuan, and Guizhou Provinces.

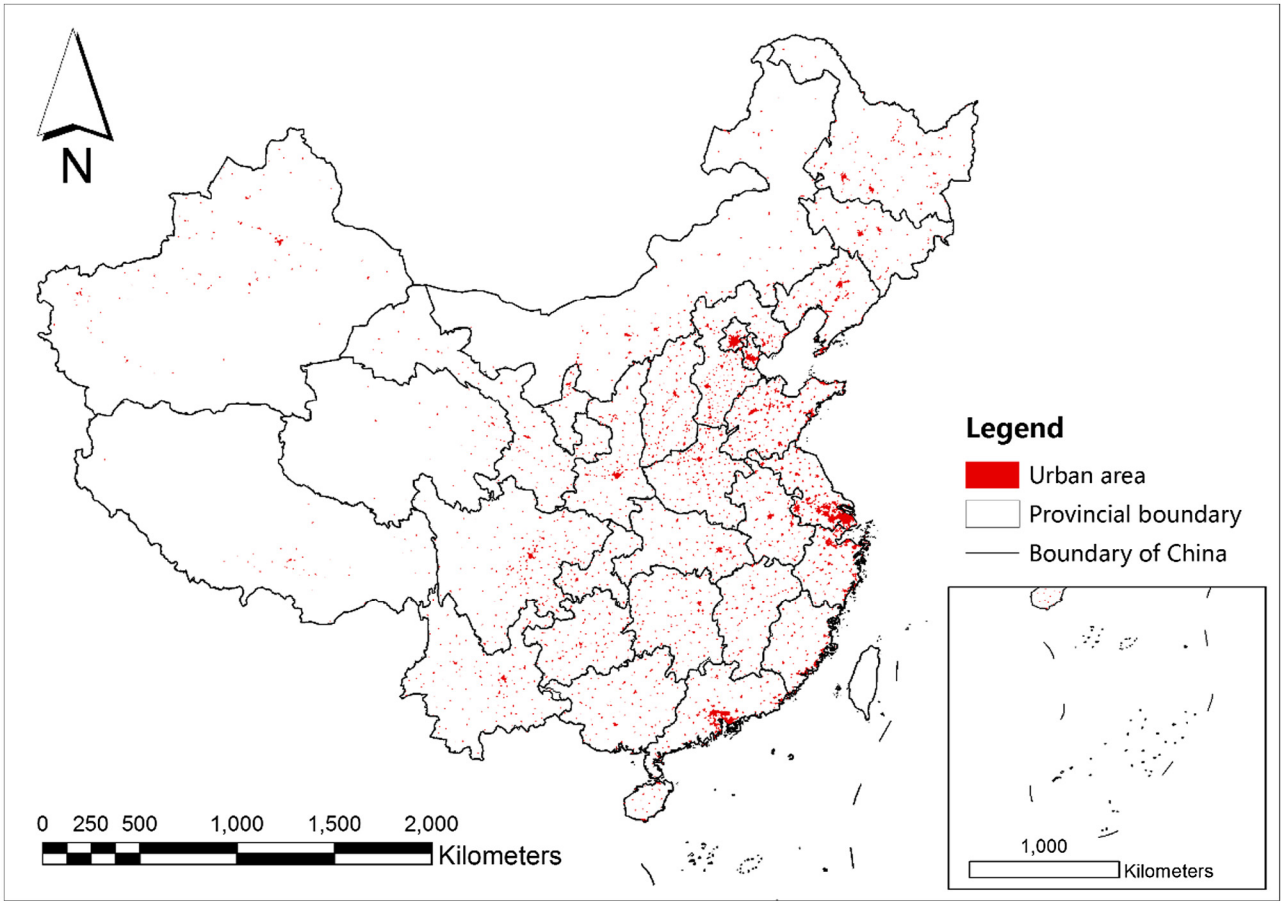


**Fig. 5.** Urban areas on the mainland of China.

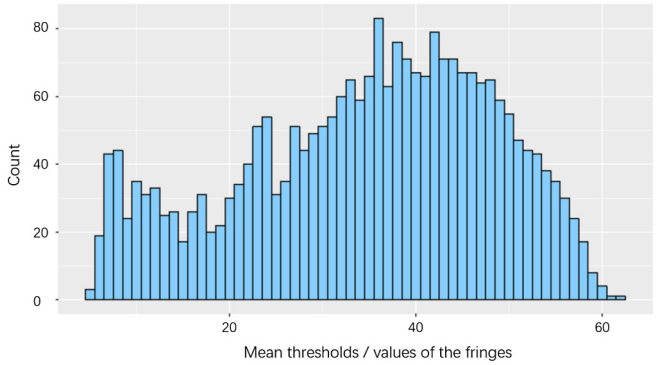


**Fig. 6.** Histogram of mean thresholds of urban patches at the prefecture level. The mean threshold of an urban patch is the mean value of the brightness of the urban fringe.

### 5.2. Urban extents

Urban patches in the east and the south were bigger and tended to have more linkages among one another than those in the west and the north, which in line with the development status of cities in China. The three conspicuous continuous urban areas were all located in the east and the south (Fig. 8). The biggest one was in the Yangtze River Delta with an area of 7529 $km^2$, which included part of Shanghai, Suzhou, Wuxi, Changzhou and Taizhou. The second biggest urban patch was in the Pearl River Delta with an area of 5521, which included part of Guangzhou, Shenzhen, Dongguan, Foshan, Zhongshan and Jiangmen. The third was 2964 $km^2$, including the biggest urban patch of Beijing and part of Sanhe.

At the regional level, East China had the highest coverage (5.9%) and average size (96.1 $km^2$) of urban patches. Urban areas in the north, south and central covered 4.2%, 3.5% and 2.7% of the land, respectively. While in the west, urban areas covered less than 1% of the land (Fig. 9; Table 3).

At the provincial level, the proportion and the distribution patterns of urban areas varied greatly (Fig. 10). Except for the formal municipalities, Jiangsu, Zhejiang, Shandong and Guangdong were the top four provinces in terms of urban coverage, all of which were higher than 5%. Tibet, Qinghai, Xinjiang, Inner Mongolia, and Gansu were the five provinces that had the lowest coverage of urban areas, with each amounting to less than 1%. All of these low urban cover provinces were located in west China. Beijing, Shanghai, Jiangsu, Zhejiang, Shandong and Guangdong were municipalities or provinces that possessed higher household incomes than other regions. Urban patches in these wealthier regions were larger in size and more clustered in space (Fig. 10, a, b, c) than urban patches in provinces having lower household incomes, such as Hebei, Henan, and Hubei. Although less wealthier or powerful, these provinces did have some large urban patches that functioned as economic centers, around which smaller urban patches clustered (Fig. 10, a, e, f). Urban patches in Yunnan, Xinjiang Provinces in the west were smaller and fewer (Fig. 10, g, h).

All prefecture-level units had urban areas, but with great variation in size and proportional coverage. Shanghai, Suzhou, Beijing, Tianjin, Wuxi, Chongqing, Dongguan, Ningbo, Guangzhou, and Nanjing were the top 10 prefectures that had the highest coverage of urban areas. The urban area of Shanghai was 203 times larger than that of Tumushuke, which had the smallest urban patch in Xinjiang province. As for the proportion of urban areas, 36 prefectures had more than 10% of their area as urban coverages, while 63 prefectures had less than 1% of urban

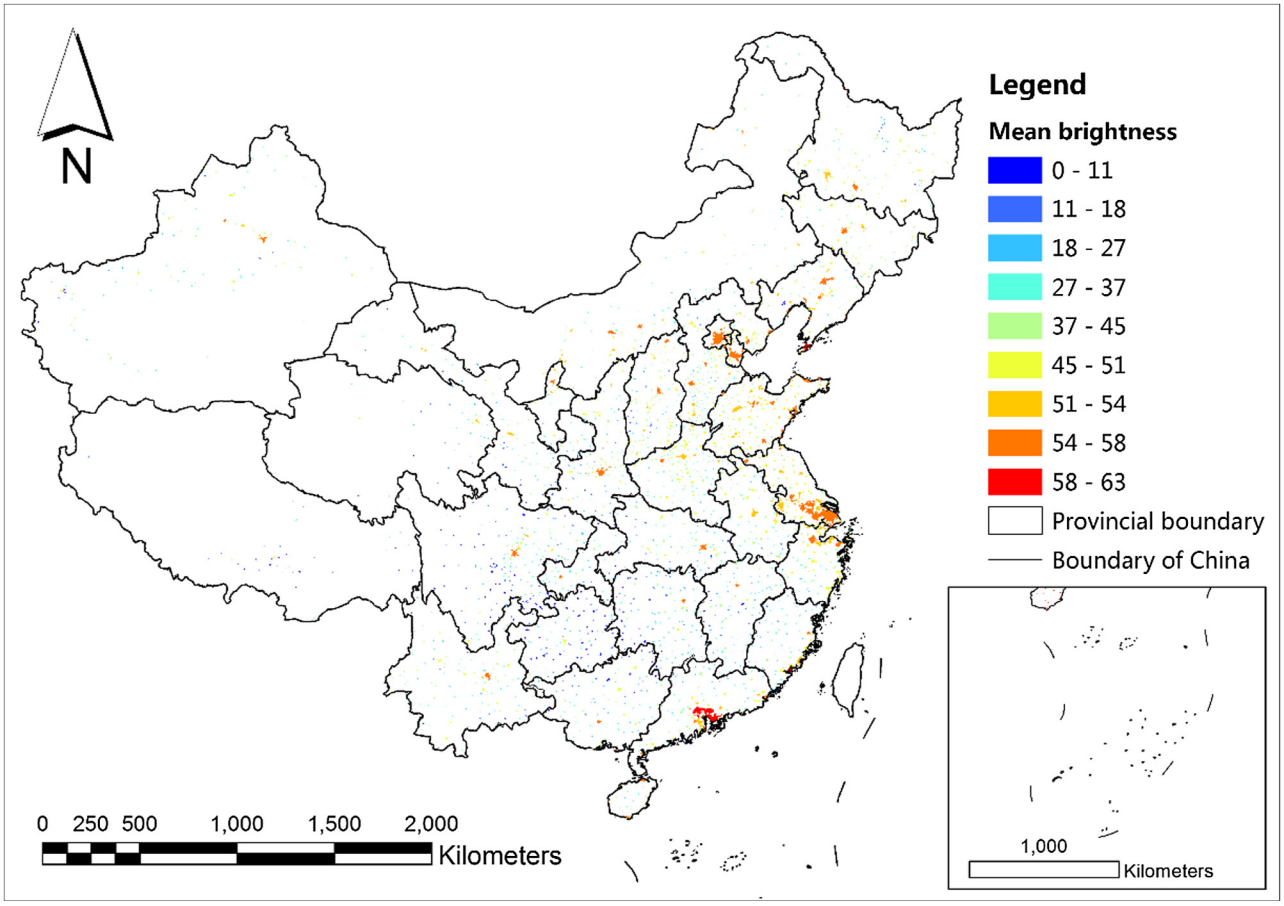


**Fig. 7.** Mean thresholds of urban patches at the prefecture level across China. Urban patches in coastal regions and capital cities had higher values of thresholds.

areas. Dongguan, Shenzhen, Shanghai and Zhongshan were the top 4 prefectures that had the highest proportion of urban areas, amounting to more than 40%. Ali, Naqu, Yushu, Alashan, Guoluo, Rikaze, Haixi, Bayin, Hetian, Linzhi and Hami, in the west of China, had less than 0.1% of the urban coverage.

### 5.3. Accuracy assessment

On the mainland China, all 31 provincial capitals, 323 out of 332 prefecture-level cities, and 2619 out of 2880 county-level urban patches were successfully detected using our new methodology for urban mapping (Fig. 2). Some cities that were not successfully detected are located in regions of no lights at night, such as cities in Tibet. We also noticed that some urban dots from Baidu Maps were distant from human settlements, which also caused errors of our detection. The accuracy of the detection for provincial capitals, prefecture-level cities and county-level cities were 100%, 97.3%, and 91.0%, respectively.

The derived urban extents and areas of the developed land inside the urban areas showed significant correlations (Fig. 11, A, r = 0.986, $P < 0.01$, $R^2 = 0.97$). The slope of the regression line was 0.57, because we considered spaces such as parks and water bodies within cities to be part of urban areas and these features covered a large proportion of land inside urban areas. In addition, the land cover data have a resolution of 90 m, that is, 10 times finer than the nighttime light data. Therefore, the relationship should not generate a slope of 1 even if parks, water bodies and other land cover types are excluded.

Urban areas delineated through our method were different from urban patches derived from land cover data in the urban boundary dataset, but had significant correlations with them (Fig. 2; Table 2; Fig. 11, B, r = 0.95, $P < 0.01$, $R^2 = 0.91$). The slope of the regression line was 0.77 rather than 1, because urban areas were derived through approaches based on different definitions of the urban, and the data have different spatial resolutions. Nighttime light data have a resolution of 1000 m while the land cover data were derived from 30 m Landsat images.

We compared our results with the modified DMSP-OLS data in which the blooming and saturation effects have been largely removed through the SEAM model (Cao et al., 2019). The model also enhanced the brightness of roads and small scattered non-urban regions, such as some transportation spots, industrial lands and villages (Fig. 12). The results showed that the blooming effects could hardly influence our urban mapping results (Fig. 12). Our mapping results matched well with those bright urban regions in the nighttime light map after applying the SEAM model. Although we lose a few urban patches, the small scattered non-urban patches are not recognized as urban areas using our mapping approach.

## 6. Discussion

### 6.1. Comparisons with previous studies

Most urban mapping studies based on the nighttime light data prefer to use land cover as reference to conduct urban mapping, and regard urban areas as impervious surfaces or developed land (Chen et al., 2019). Some of these studies stated that they aimed to recognize built-up areas using the nightlights (Shi et al., 2014; Su et al., 2015; Xie & Weng, 2016), in which case they excluded green infrastructure and water that are also urban elements. Some other studies used proportions of the impervious surface inside the mapping grids to define urban areas (Zhou et al., 2014, 2018). The mapping grids are usually squares

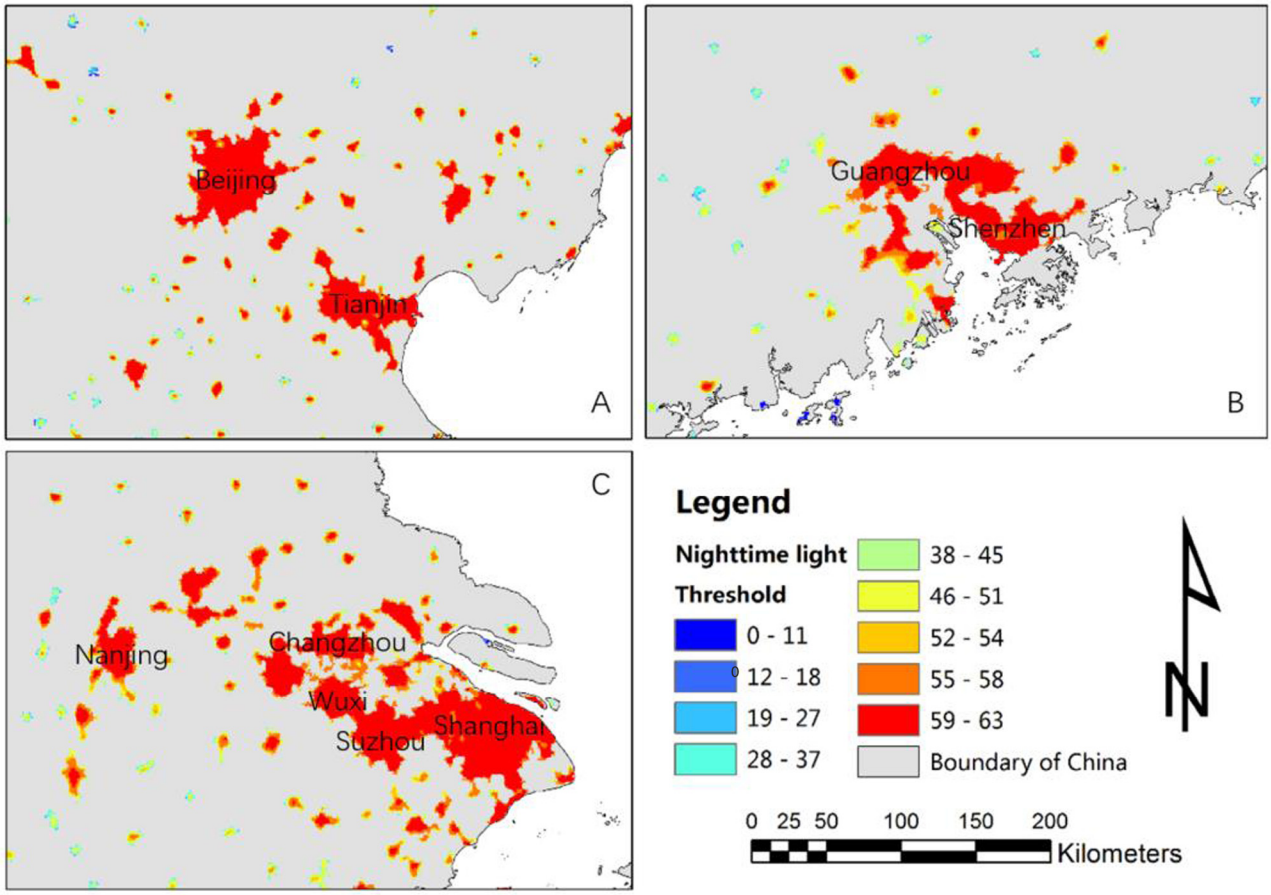


**Fig. 8.** Thresholds in three major urban megaregions in China. Thresholds of the fringes also showed connections among administratively different urban patches in megaregions. A: Beijing-Tianjin-Tangshan megaregion. B: the Pearl River Delta megaregion. C: the Yangtze River Delta megaregion.

with a size of hundred meters times hundred meters. Some studies did not mention their urban definitions but compared the mapping results with those derived from land cover data (Yang et al., 2013). The comparisons between results derived from nightlights and land covers always used the latter as a standard. However, the delimitation of the urban based on nightlights is not necessarily equivalent to the developed land or impervious surfaces (Zou et al., 2017).

Previous thresholding methods are likely to overestimate the size of big cities while underestimating the size of small cities. This may be due to their references of impervious surfaces, since the percentages of impervious surfaces at fringes in big cities are often higher than those in small cities. However, our mapping approach is able to compensate for the blooming effects of big cities, but does not work very well for small cities or dark towns (Fig. 12). We think this is due to the hypothesis and data we used. Small cities and dark towns show slight differences between urban centers and surrounding patches, so it is difficult to detect the differences theoretically. In addition, the coarse resolution of the DMSP-OLS data (1000 m) also increase the difficulty in mapping small urban patches, since there would be more mismatches in the edges. It is possible to use different grouping parameters for cities of different sizes, but this procedure would require visual comparisons and manual selections, which goes against our major goal of dividing relatively-urban regions using the dataset itself rather than making manual corrections.

The major difference between our study and previous approaches using the nighttime light data is the perspective of urban areas. Previous methods used NDVI, water masks, high resolution classification maps, topography, census data, and many other ancillary datasets to translate nighttime light into urban extents (Cheng et al., 2016; Liu et al., 2012; Tan, 2016; Townsend & Bruce, 2010; Xie & Weng, 2016; Zhou et al., 2015, 2014). Most of these urban mapping studies, regardless of what ancillary data they used - whether land cover maps, population distribution, or economic categories - were actually translating nighttime light data into other types of data and using the land cover data as reference. Such translation relies on the perspective that there is only one standard to map the urban and only one type of urban boundaries existing in reality.

In our method, the recognition of urban fringes depends on the night lights themselves, without setting potential boundaries referring to other types of data. The results of linkages among urban patches that derived from different urban centers will not be separated by manual preference or prior impressions. For example, the major urban patch of Beijing city consisted of patches from Dongcheng, Xicheng, Haidian, Chaoyang and eight other districts in 2010. Instead of physically relating to the other four smaller urban patches distributed inside Beijing municipality, the major urban patch of Beijing city was connected with the urban patch in Yanjiao and Sanhe, towns in the east to Beijing municipality.

There are similar efforts to convey diverse perspectives of urban regions in other parts of the world. Zhou et al. (2018) developed an approach to map urban areas globally with only DMSP-OLS data themselves. García-Palomares, Gutiérrez, and Mínguez (2015) conducted an urban mapping of spatial human activities from locals and tourists in several European cities through geotagged photographs, implying that local residents and tourists perceived the same city differently. Aiello, Schifanella, Quercia, and Aletta (2016) used picture tags to map Barcelona and London into sound maps, depicting unfamiliar urban regions from visual buildings and streets. Uchiyama and Mori (2017) reviewed literature showing that cities could be defined

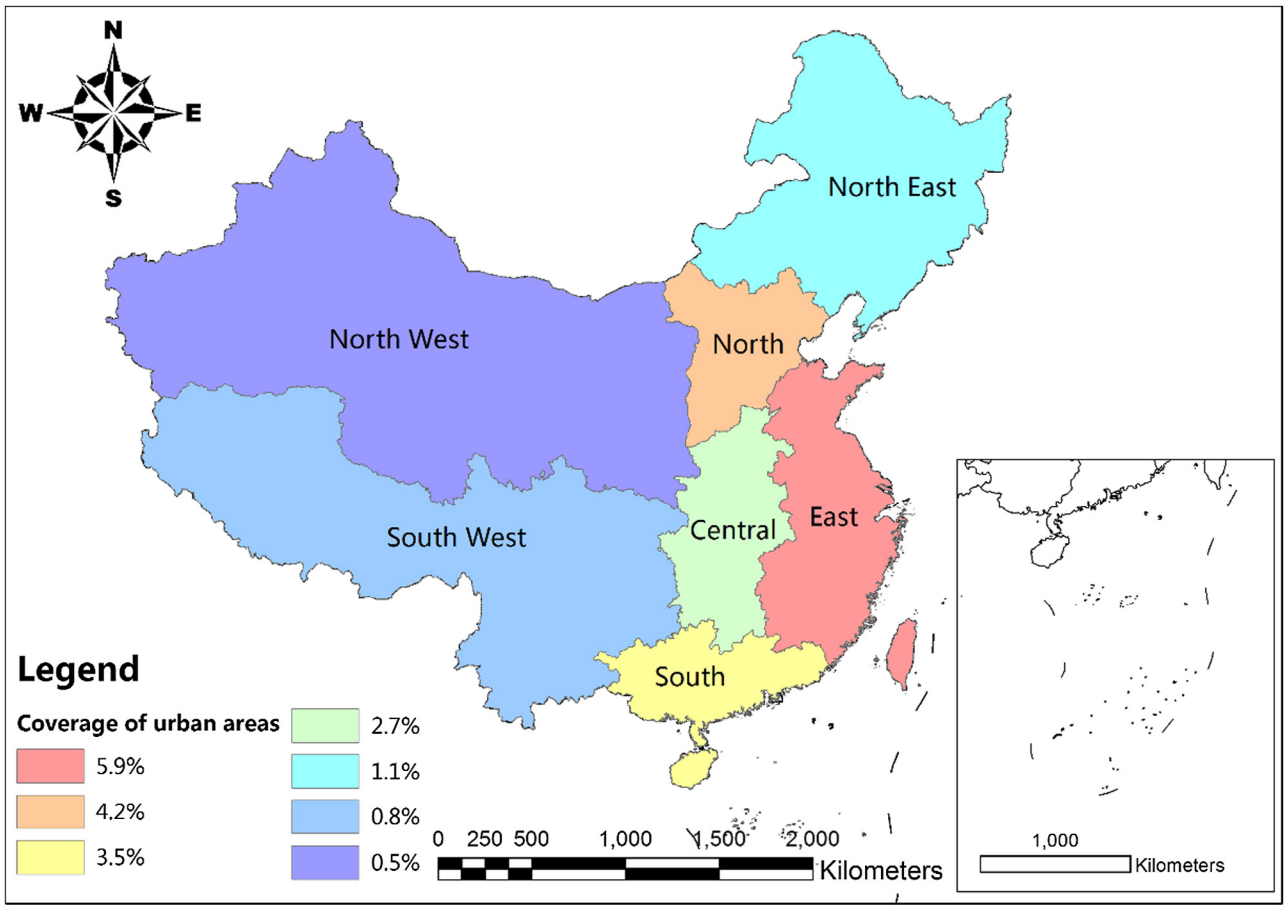


**Fig. 9.** Geographical regions of China and their urban coverages.

**Table 3**
Attributes of urban areas in seven geographical regions.

| Region | Proportion of the total area | Average size ($km^2$) | Maximum size ($km^2$) | Mean brightness of the light | Standard deviation of the light |
|---|---|---|---|---|---|
| East | 5.9% | 96.1 | 7529 | 42.9 | 11.7 |
| North | 4.2% | 69.2 | 2964 | 43.2 | 10.2 |
| South | 3.5% | 76.7 | 6065 | 35.3 | 13.6 |
| Central | 2.7% | 50.9 | 681 | 34.5 | 11.9 |
| North-east | 1.1% | 57.6 | 779 | 45.3 | 9.7 |
| South-west | 0.8% | 43.3 | 693 | 27.4 | 14.2 |
| North-west | 0.5% | 45.1 | 1158 | 37.2 | 13.5 |

and delineated in practice based on landcover, night lights, and population, and the results varied greatly according to different practical criteria.

In order to virtually show the similarities and differences between our urban mapping results and previous studies, we further conducted urban mapping in China in 2005 to compare our results with those delineated by Zhou et al. (2014). In general, our mapping results matched pretty well with their results, and we both delineated most of the urban areas in the Beijing-Tianjin-Hebei region (Fig. 13). We delineated 183 urban patches using our approach, while the number of urban patches in the same region is 214 using Zhou's method. Our methods extracted fewer but more connected urban patches than those from Zhou et al. (2014), which we think is due to the different definition of the urban in two methods. Zhou's approach detected more urban patches, but some small scattered patches might be non-urban patches considering their sizes or functions. Our approach detected fewer urban patches, and most of them were urban areas for sure, but we might lose some relatively small and dark urban areas.

Although these two methods can delineate most of the urban areas in the Beijing-Tianjin-Hebei region, they might both miss some of the urban areas in this region. There are 206 county points in this region currently. Based on the ways of China developing and managing urban areas, there should be fewer than 206 urban areas that have official names. In Zhou's mapping results, there are 157 urban patches overlapping with county points, and 14 county points have no urban patches to match with. In our mapping results, there are 147 urban patches overlapping with county points, and 22 county points have no urban patches to match with.

### 6.2. Advantages and disadvantages of the "relatively urban" mapping approach

Our study used the idea of "relatively urban" to map urban extents. This method delineated urban fringes according to a grouping algorithm, which was conducted on every urban center in China based on the nighttime light data. It classified patches into a relatively urbanized group where objects were similar to the bright urban nightlife centers, and a relatively non-urban group that was close to dark rural or uninhabited areas.

We admit that our mapping results are coarse, because the blooming effects cannot be erased completely using the grouping method with the 1000 m DMSP/OLS data as mentioned earlier. However, it is acceptable to use this dataset for urban mapping at the regional scale (Fig. 12). Another important factor influencing our mapping result is the quality of the administrative boundaries. If the units do not update with the latest adjustment (Sections 2 and 3.2), our approach might fail to detect some of the newly-emerged urban patches. Locations of cities could be

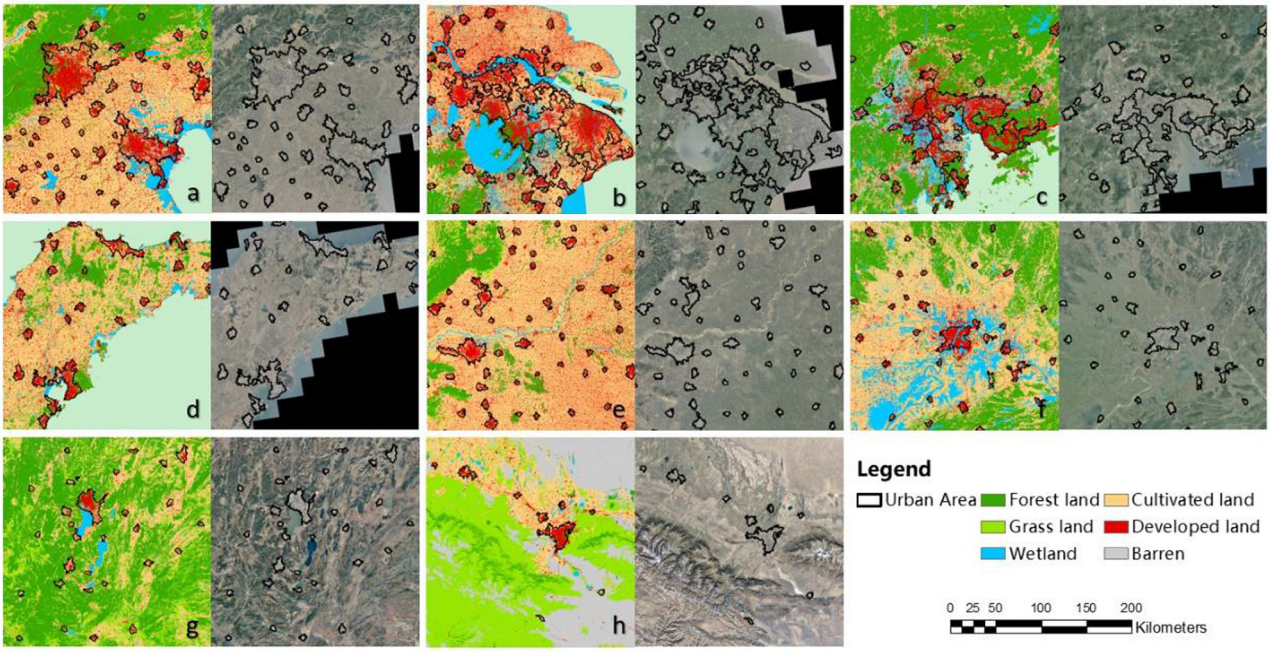


**Fig. 10.** Delineated urban areas mapped on the land cover and remote sensing images in 2010. Continual urban patches are segmented by prefecture-level boundaries. a: Beijing, Tianjin and Hebei Province; b: Shanghai, Jiangsu and Zhejiang Provinces; c: Guangdong Province; d: Shandong peninsula; e: Henan Province; f: Hubei Province; g: Yunnan Province; h: Xinjiang Province.

used as additional data to help map urban regions, but which would weaken our original attempt to promote a simple method using as few ancillary data as possible. Meanwhile, the accuracy of locations of cities might cause other problems (Section 5.3).

Nevertheless, our major point is to provide methodologies to efficiently map urban areas based on different perspectives. Our method can detect and map urban areas under different definitions efficiently, because the basic ideas of the urban detection and the grouping algorithm are simple and direct. Based on the criteria considering both local and regional characteristics, this method is usable for comparative analysis at large spatial extents or long-term temporal scales.

The object-based approach with a grouping algorithm we developed in this paper provides a way to recognize relatively urban regions using different datasets. With the development of techniques of remote sensing and widely used geo-tagged data, previous methods or parameters that worked well on DMSP-OLS data would have to be revised to work on new data. However, our approach does not set up thresholds or parameters in advance, and the grouping process is based on the dataset itself: therefore it has the potential to be applied to any type of data. For instance, we used the nighttime light data to map urban regions with more lights and electric-based residential and commercial nightlives. We can also use the social-media data, location-tagged data, or perceptions about the city with the same approach to describe urban regions with different characteristics or lifestyles.

### 6.3. Knowledges of the urban areas are necessary for urban mapping

The knowledge of how urban areas are administered or organized in the study region helped to choose the operating scale for urban mapping (e.g. Box 1). Urban areas in different countries or regions might

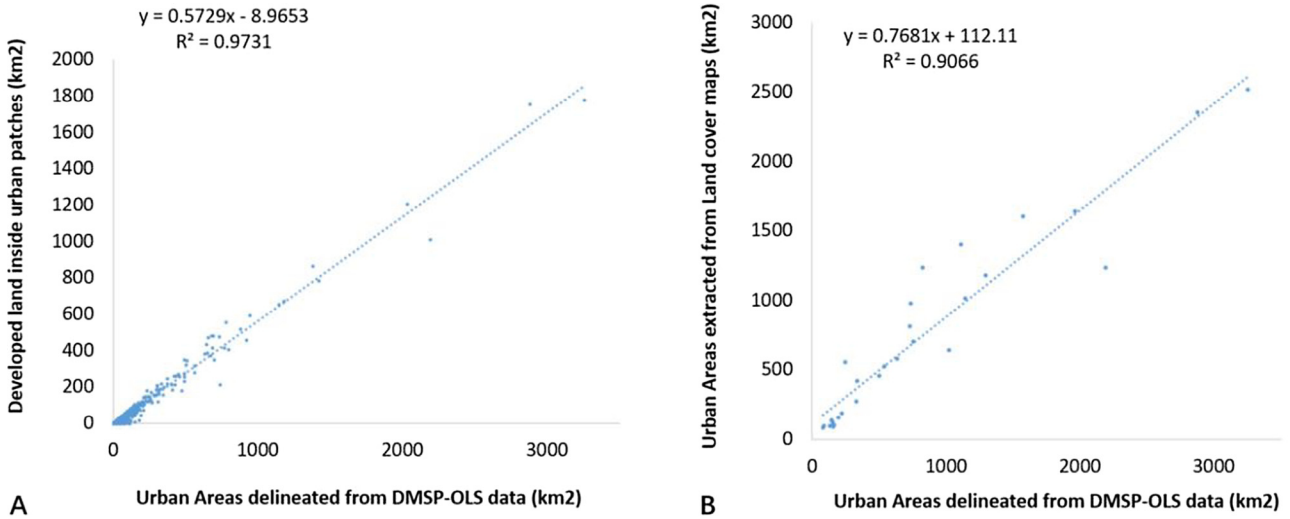


**Fig. 11.** A. Relationship between urban areas delineated from the DMSP-OLS data and total areas of the developed land inside those urban patches. B. Relationships between urban areas delineated from the DMSP-OLS data and those from the urban boundary dataset.

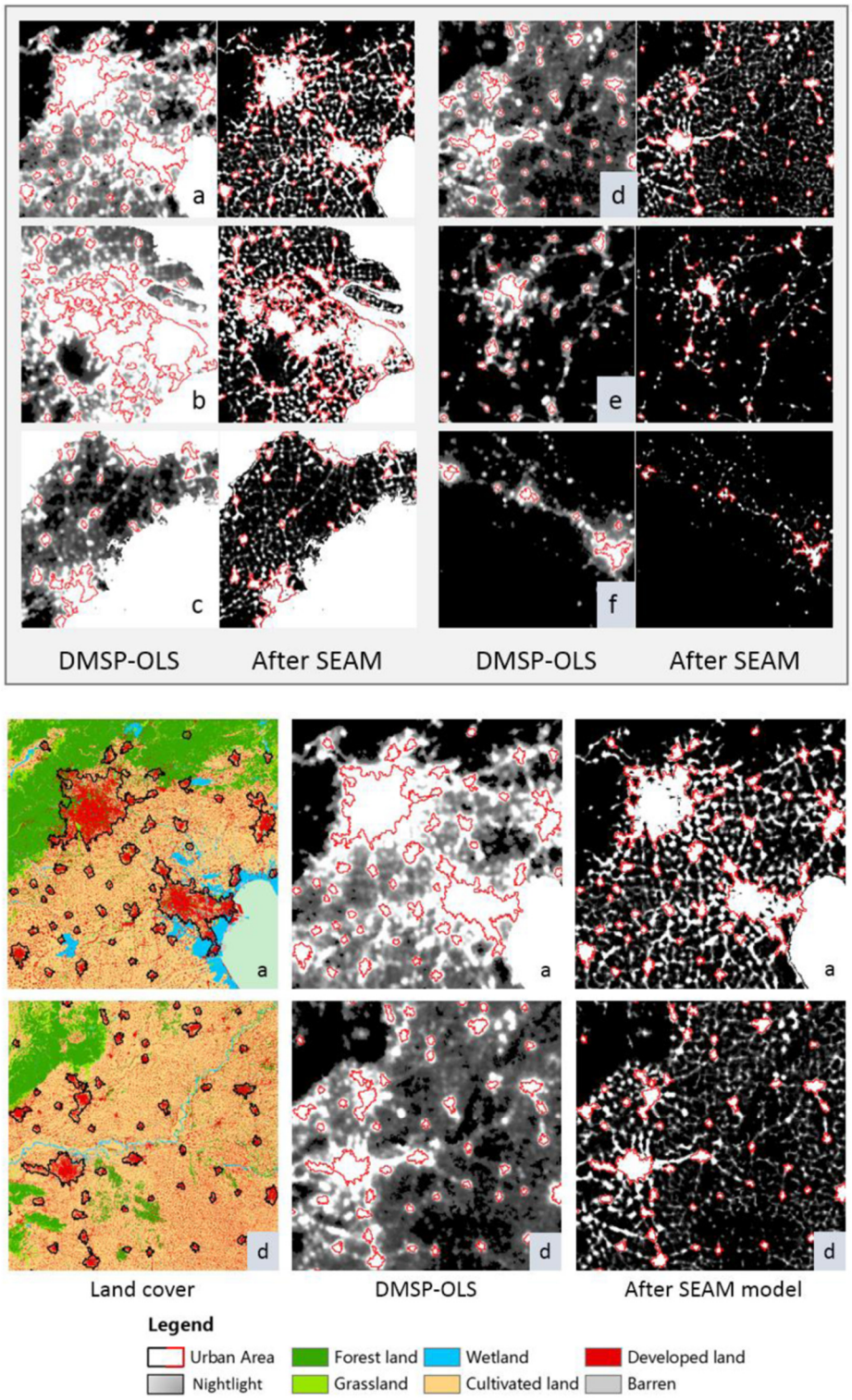


**Fig. 12.** Urban mapping results overlapped with the original DMSP-OLS map, modified DMSP-OLS data (After SEAM; SEAM is a model to mitigate the blooming and saturation of the DMSP-OLS data, Cao et al., 2019), and the land cover maps. a: Beijing, Tianjin and Hebei Province; b: Shanghai, Jiangsu and Zhejiang Provinces; c: Shandong peninsula; d: Henan Province; e: Yunnan Province; f: Xinjiang Province.

obey different rules of organization, which gives additional information on where urban areas might emerge. In China, either big cities or small towns are controlled by the basic administrative units at the county level, which is beneath the prefecture level. That is, every urban patch is controlled by a county-level government, and urban patches that are not physically connected might belong to the same prefecture-level city or municipality administratively. For example, Tianjin municipality sets up a new costal county to administer its newly developed urban patch near the harbor, which is far from Tianjin downtown.

The knowledge of how urban patches spread helped to decide the grouping algorithm. Some urban patches in China break through administrative boundaries to connect with one another, but they do not necessarily belong to the same city administratively. Therefore, it is not proper to constrain an urban patch from sprawling out of its

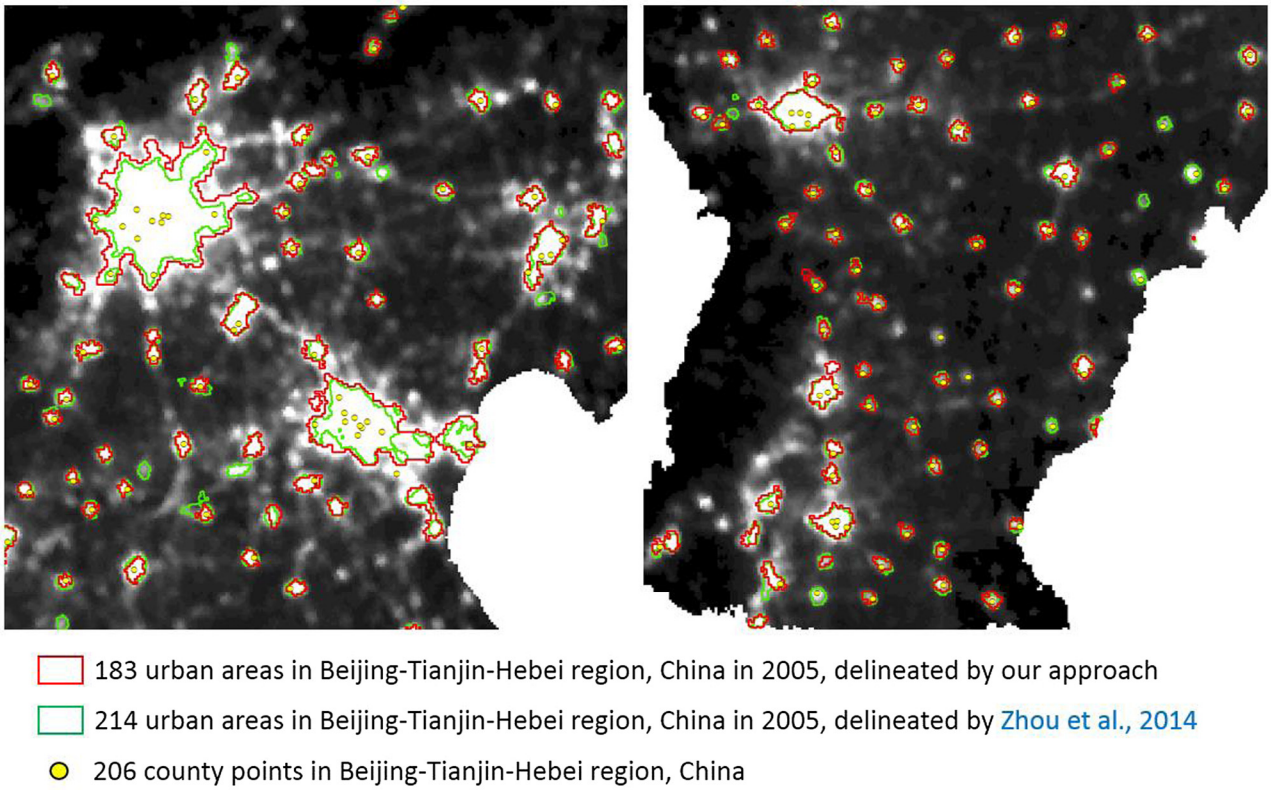


**Fig. 13.** Urban mapping results in 2005 based on our approach, compared with urban areas delineated from Zhou et al., 2014.

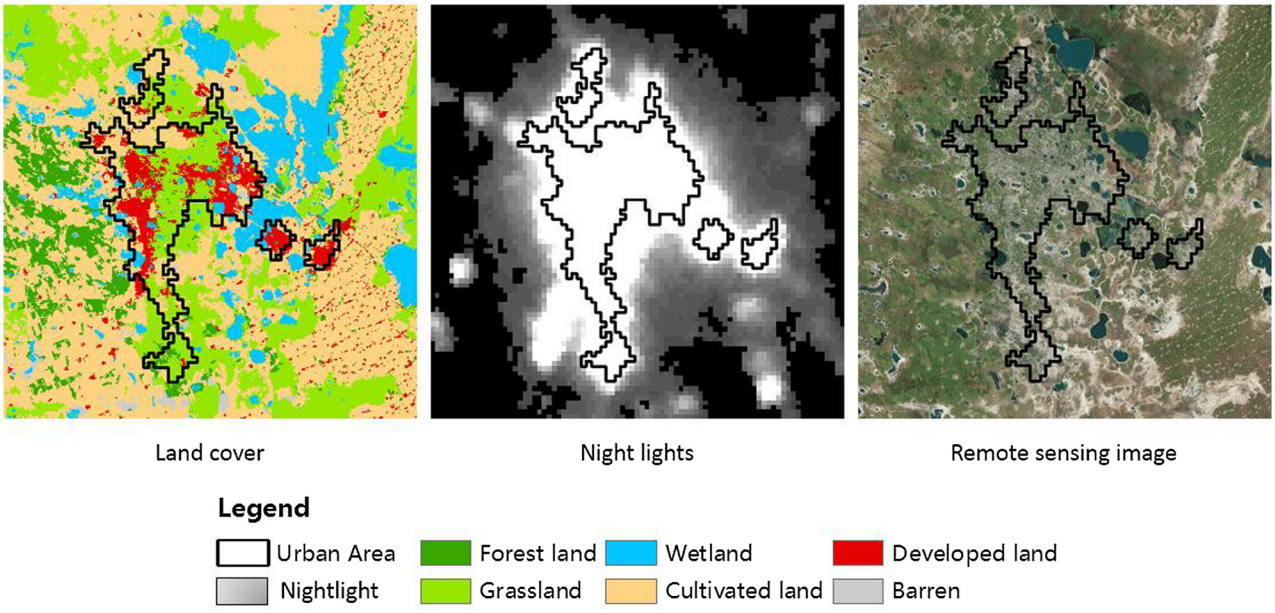


**Fig. 14.** The land cover, night lights, and the original remote sensing images of Daqing, a city based on oilfields in the northeast of China. Some classification errors can be found in the land cover map in the largest middle patch compared with original image on the right. There might be gas flares in the map of night lights.

administrative boundary, and we did not set up such rules in the grouping algorithm. Examples include the urban megaregions in the Pearl river delta and in the Yangtze River Delta (Figs. 8, B, C; 10, b, c).

Another important issue is to understand that urban areas differ spatially and temporally. Knowing what characteristics of the urban can be derived from specific datasets would support meaningful urban mapping. We used the nighttime light data to map urban areas in China, because we think it is possible to distinguish urban areas from this dataset. We assume that people in most cities in China would engage in active nighttime activities illuminated by artificial light that spills into the sky. Such active night lifestyle may well be a symbol of urban life, leisure, and consumption (Shaw, 2014). However, such assumptions might not be applicable in some other parts of the world or some certain types of cities where nighttime activities are not popular. Therefore, the specific criteria used for urban mapping should be based on local characteristics.

### 6.4. Diverse perspectives and integration are needed for understanding of the urban

In general, most people can depict images about the urban in their heads very easily – tall buildings and busy streets. Under the same logic, non-urban regions could be depicted as places with flowing rivers and green trees. Such inherited impressions may encourage researchers to employ the visual physical differences of the grey and green as criteria to distinguish urban and non-urban places. However, are there unambiguous urban boundaries in reality? If so, what do such boundaries separate, or in other words, what do such separated urban or non-urban regions represent?

If we take a closer look, we may find land cover and nighttime light data tell different stories. The easiest way to understand the difference is to look at the concrete or grey surfaces on Earth. Although urban and rural areas both have structures of concrete and impervious surfaces which look the same as red pixels in land cover maps, the concrete surfaces have different appearances in nighttime light maps (Figs. 10 and 14). Similarly, regions with similar values of the brightness look different on land cover maps (Fig. 14). Shall we understand these differences as deviations caused by different datasets, or shall we admit that there are different legitimate ways of viewing the urban?

Urban areas have diverse features, sizes, forms and functions, which makes the urban area hard to define and of no universally accepted definition (Aubrecht, Gunasekera, Ungar, & Ishizawa, 2016; Chen et al., 2019; Huang et al., 2016; Klotz et al., 2016; Pickett & Zhou, 2015; Sutton, 2003). Current urban studies imply that urban systems are complex and consist of many kinds of spatial mosaics (Grove et al., 2015), and the urban should be regarded as a process rather than a universal bounded unit (Brenner & Schmid, 2015). Since there is no single distinct line between the urban and its surrounding regions (McIntyre et al., 2000), an urban boundary should be recognized for each type of mosaic or features according to the specific questions guiding a research project. In addition to the visual physical structures of buildings and roads, other urban functions and human perceptions can also be used to understand urban areas (Gandy, 2012; Lefebvre, 2003; Monte-Mór, 2005). For instance, under the perspective of daily commuting, the urban areas of New York city or Shanghai could be much larger than expectations, or at least much larger than the concrete developed land delineated through the land cover types.

Integrated datasets are required to define and detect urban areas (Cai, Huang, & Song, 2016; Elvidge et al., 2009). If urban areas are combinations of complex mosaics, as mentioned earlier, integrated datasets will be important. For example, the land cover shows the pattern or mosaics of buildings, pavements, and green infrastructures, the nighttime light data gives clues on urban settlements and transportation, while the social-media and location-tagged data describes preferences and human daily activities. Thinking of how these mosaics combined with each other, we may find a more convincing way of understanding the urban and linkages among places, which is vital for reasonable urban planning and management.

## 7. Conclusion

We propose a flexible approach that can be applied on datasets that describe aspects of the urban from diverse perspectives, which meets the demand of up-to-date urban mapping approaches and current theoretical understanding of the urban. The specific method we use in this paper can delineate defined urban areas efficiently at the regional scale through nighttime light data and county-level administrative units in China. The method has a low requirement for ancillary data and is usable for comparative analysis at large spatial extents or long-term temporal scales.

We do not set urban centers using points of interest (POI) data or through manual selections, rather, all the initial urban centers were detected using the same criteria across the whole country. Without the procedure of using high resolution remote sensing images, our method saves a large amount of time and labor. We believe this method can be used in other places to map urban areas with nighttime lights or other datasets that describe some characteristics of the urban. One detail of using this approach in other places or to reveal temporal patterns is that the mapping unit should be decided based on local conditions. For example, the dataset of Places could be used as the unit for urban detection in the United States.

Because urban mosaics are complex and multidimensional, there is no single way to define or delineate urban areas. Therefore, urban boundaries must be drawn based on specific characteristics according to research questions or management applications. Urban mapping that integrates local knowledges such as the administrative organization of human settlements can help enhance the understanding of urbanization in the region of interest. Our approach of urban mapping lays the basis for an integrated perception of urban mosaics, which is necessary for urban planning and management. Therefore, we believe it is useful for promoting urban studies.

## Acknowledgements

This research was funded by “Developing key technologies for establishing ecological security patterns at the Beijing-Tianjin- Hebei urban megaregion” of the National Key Research and Development Program (2016YFC0503004), the Key Research Program of Frontier Sciences, CAS (QYZDB-SSW-DQC034), and the National Natural Science Foundation of China (Grant Nos. 41590841 & 41771203). Thank Dr. Yuyu Zhou from Iowa State University for providing us with their urban mapping results. Thank Dr. Xiaolin Zhu from the Hong Kong Polytechnic University and Yang Hu from Beijing Normal University for providing the SEAM model. We also thank the editor and reviewers, who gave valuable comments and suggestions on this manuscript.

## References

Aiello, L. M., Schifanella, R., Quercia, D., & Aletta, F. (2016). Chatty maps: Constructing sound maps of urban areas from social media data. *Royal Society Open Science, 3*(3), 150690.

Aronson, M. F. J., La Sorte, F. A., Nilon, C. H., Katti, M., Goddard, M. A., Lepczyk, C. A., ... Winter, M. (2014). A global analysis of the impacts of urbanization on bird and plant diversity reveals key anthropogenic drivers. *Proceedings of the Royal Society B, 281*, 20133330. https://doi.org/10.1098/rspb.2013.3330.

Aubrecht, C., Gunasekera, R., Ungar, J., & Ishizawa, O. (2016). Consistent yet adaptive global geospatial identification of urban–rural patterns: The iURBAN model. *Remote Sensing of Environment, 187*, 230–240. https://doi.org/10.1016/j.rse.2016.10.031.

Bennett, M. M., & Smith, L. C. (2017). Advances in using multitemporal night-time lights satellite imagery to detect, estimate, and monitor socioeconomic dynamics. *Remote Sensing of Environment, 192*, 176–197. https://doi.org/10.1016/j.rse.2017.01.005.

Brenner, N., & Schmid, C. (2014). The ‘urban age’ in question. *International Journal of Urban and Regional Research, 38*(3), 731–755.

Brenner, N., & Schmid, C. (2015). Towards a new epistemology of the urban? *City, 19*(2–3), 151–182.

Cadenasso, M. L., Pickett, S. T. A., & Schwarz, K. (2007). Spatial heterogeneity in urban ecosystems: Reconceptualizing land cover and a framework for classification. *Frontiers in Ecology and the Environment, 5*, 80–88. https://doi.org/10.1890/1540-9295(2007) 5[80:SHIUER]2.0.CO;2.

Cai, J., Huang, B., & Song, Y. (2016). Using multi-source geospatial big data to identify the structure of polycentric cities. *Remote Sensing of Environment.* https://doi.org/10.1016/j.rse.2017.06.039.

Cao, X., Chen, J., Imura, H., & Higashi, O. (2009). A SVM-based method to extract urban areas from DMSP-OLS and SPOT VGT data. *Remote Sensing of Environment, 113*, 2205–2209. https://doi.org/10.1016/j.rse.2009.06.001.

Cao, X., Hu, Y., Zhu, X., Shi, F., Zhuo, L., & Chen, J. (2019). A simple self-adjusting model for correcting the blooming effects in DMSP-OLS nighttime light images. *Remote Sensing of Environment, 224*, 401–411.

Chen, Z., Yu, B., Zhou, Y., Liu, H., Yang, C., Shi, K., & Wu, J. (2019). Mapping global urban areas from 2000 to 2012 using time-series nighttime light data and MODIS products. *IEEE Journal of Selected Topics in Applied Earth Observations and Remote Sensing, 12*(4), 1143–1153.

Cheng, Y., Zhao, L., Wan, W., Li, L., Yu, T., & Gu, X. (2016). Extracting urban areas in China using DMSP/OLS nighttime light data integrated with biophysical composition information. *Journal of Geographical Sciences, 26*, 325–338. https://doi.org/10.1007/s11442-016-1271-6.

Elvidge, C. D., Baugh, K., Zhizhin, M., & Hsu, F. C. (2013). Why VIIRS data are superior to DMSP for mapping nighttime lights. *Proceedings of the Asia-Pacific Advanced Network,*

*62–69*. https://doi.org/10.7125/APAN.35.7.
Elvidge, C. D., Imhoff, M. L., Baugh, K. E., Hobson, V. R., Nelson, I., Safran, J., ... Tuttle, B. T. (2001). Night-time lights of the world: 1994–1995. *ISPRS Journal of Photogrammetry and Remote Sensing, 56*, 81–99. https://doi.org/10.1016/S0924-2716(01)00040-5.
Elvidge, C., Sutton, P., Tuttle, B., Ghosh, T., & Baugh, K. (2009). Global Urban Mapping based on Nighttime Lights. *Global Mapping of Human Settlement: Experiences, Datasets and Prospects*, 129–145. https://doi.org/10.1201/9781420083408-c6.
Elvidge, C. D., Zhizhin, M., Hsu, F. C., & Baugh, K. E. (2013). VIIRS nightfire: Satellite pyrometry at night. *Remote Sensing, 5*, 4423–4449. https://doi.org/10.3390/rs5094423.
Fan, S., Li, L., & Zhang, X. (2012). Challenges of creating cities in China: Lessons from a short-lived county-to-city upgrading policy. *Journal of Comparative Economics, 40*, 476–491. https://doi.org/10.1016/j.jce.2011.12.007.
Gandy, M. (2012). Where does the city end?? *Architectural Design, 82*(1), 128–1119. https://doi.org/10.1002/ad.1363.
García-Palomares, J. C., Gutiérrez, J., & Mínguez, C. (2015). Identification of tourist hot spots based on social networks: A comparative analysis of European metropolises using photo-sharing services and GIS. *Applied Geography, 63*, 408–417.
Ginzarly, M., Roders, A. P., & Teller, J. (2018). Mapping historic urban landscape values through social media. *Journal of Cultural Heritage*.
Grimm, N. B., Faeth, S. H., Golubiewski, N. E., Redman, C. L., Wu, J., Bai, X., & Briggs, J. M. (2008). Global change and the ecology of cities. *Science (80-.), 319*, 756–760. https://doi.org/10.1126/science.1150195.
Grove, J. M., Cadenasso, M., Pickett, S. T., Burch, W. R., & Machlis, G. E. (2015). *The Baltimore School of Urban Ecology: Space, scale, and time for the study of cities.* Yale University Press.
He, C., Shi, P., Li, J., Chen, J., Pan, Y., Li, J., ... Toshiaki, I. (2006). Restoring urbanization process in China in the 1990s by using non-radiance-calibrated DMSP/OLS nighttime light imagery and statistical data. *Chinese Science Bulletin, 51*, 1614–1620. https://doi.org/10.1007/s11434-006-2006-3.
Henderson, M., Yeh, E. T., Gong, P., Elvidge, C., & Baugh, K. (2003). Validation of urban boundaries derived from global night-time satellite imagery. *International Journal of Remote Sensing, 24*, 595–609. https://doi.org/10.1080/01431160304982.
Huang, X., Schneider, A., & Friedl, M. A. (2016). Mapping sub-pixel urban expansion in China using MODIS and DMSP/OLS nighttime lights. *Remote Sensing of Environment, 175*, 92–108. https://doi.org/10.1016/j.rse.2015.12.042.
Imhoff, M. L., Lawrence, W. T., Stutzer, D. C., & Elvidge, C. D. (1997). A technique for using composite DMSP/OLS "city lights" satellite data to map urban area. *Remote Sensing of Environment, 61*, 361–370. https://doi.org/10.1016/S0034-4257(97)00046-1.
Klotz, M., Kemper, T., Geiß, C., Esch, T., & Taubenböck, H. (2016). How good is the map? A multi-scale cross-comparison framework for global settlement layers: Evidence from Central Europe. *Remote Sensing of Environment, 178*, 191–212. https://doi.org/10.1016/j.rse.2016.03.001.
Lefebvre, H., 2003. The urban revolution. U of Minnesota Press. Original edition, 1970.
Li, X., & Zhou, Y. (2017). Urban mapping using DMSP/OLS stable night-time light: A review. *International Journal of Remote Sensing, 38*, 6030–6046. https://doi.org/10.1080/01431161.2016.1274451.
Liu, Z., He, C., Zhang, Q., Huang, Q., & Yang, Y. (2012). Extracting the dynamics of urban expansion in China using DMSP-OLS nighttime light data from 1992 to 2008. *Landscape and Urban Planning, 106*, 62–72. https://doi.org/10.1016/j.landurbplan.2012.02.013.
Lu, D., Tian, H., Zhou, G., & Ge, H. (2008). Regional mapping of human settlements in southeastern China with multisensor remotely sensed data. *Remote Sensing of Environment, 112*, 3668–3679. https://doi.org/10.1016/j.rse.2008.05.009.
Ma, T., Zhou, Y., Zhou, C., Haynie, S., Pei, T., & Xu, T. (2015). Night-time light derived estimation of spatio-temporal characteristics of urbanization dynamics using DMSP/OLS satellite data. *Remote Sensing of Environment, 158*, 453–464. https://doi.org/10.1016/j.rse.2014.11.022.
Martinuzzi, S., Gould, W. A., & Gonzalez, O. M. R. (2007). Land development, land use, and urban sprawl in Puerto Rico integrating remote sensing and population census data. *Landscape and Urban Planning, 79*(3–4), 288–297.
Mathieu, R., Aryal, J., & Chong, A. (2007). Object-based classification of Ikonos imagery for mapping large-scale vegetation communities in urban areas. *Sensors, 7*(11), 2860–2880.
McIntyre, N. E., Knowles-Yanez, K., & Hope, D. (2000). Urban ecology as an interdisciplinary field: Differences in the use of "urban" between the social and natural sciences. *Urban Ecosystems, 4*, 5–24. https://doi.org/10.1023/A:1009540018553.
Monte-Mór, R. L. (2005). What is the urban in the contemporary world? *Cadernos de Saúde Pública, 21*, 942–948.
Myint, S. W., Gober, P., Brazel, A., Grossman-Clarke, S., & Weng, Q. (2011). Per-pixel vs. object-based classification of urban land cover extraction using high spatial resolution imagery. *Remote Sensing of Environment, 115*, 1145–1161. https://doi.org/10.1016/j.rse.2010.12.017.
Ouyang, Z., Zheng, H., Xiao, Y., Polasky, S., Liu, J., Xu, W., Wang, Q., Zhang, L., Xiao, Y., Rao, E., Jiang, L., Lu, F., Wang, X., Yang, G., Gong, S., Wu, B., Zeng, Y., Yang, W., & Daily, G. C. (2016). Improvements in ecosystem services from investments in natural capital. *Science (80-.), 352*, 1455–1459. https://doi.org/10.1126/science.aaf2295.
Peng, J., Hu, Y., Liu, Y., Ma, J., & Zhao, S. (2018). A new approach for urban-rural fringe identification: Integrating impervious surface area and spatial continuous wavelet transform. *Landscape and Urban Planning, 175*, 72–79. https://doi.org/10.1016/j.landurbplan.2018.03.008.
Pickett, S. T. A., & Zhou, W. (2015). Global urbanization as a shifting context for applying ecological science toward the sustainable city. *Ecosystem Health and Sustainability, 1*, art5-art5. https://doi.org/10.1890/EHS14-0014.1.
Pu, R., Landry, S., & Yu, Q. (2011). Object-based urban detailed land cover classification with high spatial resolution IKONOS imagery. *International Journal of Remote Sensing, 32*(12), 3285–3308.
Rademacher, A., Cadenasso, M. L., & Pickett, S. T. A. (2019). From feedbacks to coproduction: Toward an integrated conceptual framework for urban ecosystems. *Urban Ecosystems, 22*(1), 65–76. https://doi.org/10.1007/s11252-018-0751-0.
Shaw, R. (2014). Beyond night-time economy: Affective atmospheres of the urban night. *Geoforum, 51*, 87–95.
Shi, K., Huang, C., Yu, B., Yin, B., Huang, Y., & Wu, J. (2014). Evaluation of NPP-VIIRS night-time light composite data for extracting built-up urban areas. *Remote Sensing Letters, 5*, 358–366. https://doi.org/10.1080/2150704X.2014.905728.
Small, C., Pozzi, F., & Elvidge, C. D. (2005). Spatial analysis of global urban extent from DMSP-OLS night lights. *Remote Sensing of Environment, 96*, 277–291. https://doi.org/10.1016/j.rse.2005.02.002.
Su, Y., Chen, X., Wang, C., Zhang, H., Liao, J., Ye, Y., & Wang, C. (2015). A new method for extracting built-up urban areas using DMSP-OLS nighttime stable lights: A case study in the Pearl River Delta, southern China. *GIScience & Remote Sensing, 52*(2), 218–238.
Sutton, P. C. (2003). A scale-adjusted measure of "Urban Sprawl" using nighttime satellite imagery. *Remote Sensing of Environment, 86*, 353–369. https://doi.org/10.1016/S0034-4257(03)00078-6.
Tan, M. (2016). Use of an inside buffer method to extract the extent of urban areas from DMSP/OLS nighttime light data in North China. *GIScience Remote Sensing, 53*, 444–458. https://doi.org/10.1080/15481603.2016.1148832.
Townsend, A. C., & Bruce, D. A. (2010). The use of night-time lights satellite imagery as a measure of Australia's regional electricity consumption and population distribution. *International Journal of Remote Sensing, 31*, 4459–4480.
Trimble Germany GmbH, 2014. Multiresolution Segmentation, in: eCognition Developer 9.0 Reference Book. pp. 64–69.
Uchiyama, Y., & Mori, K. (2017). Methods for specifying spatial boundaries of cities in the world: The impacts of delineation methods on city sustainability indices. *Science of the Total Environment, 592*, 345–356.
Wu, J., & Ding, J. (2018). Types, characteristics and tendency of county-level administrative division adjustment in China since 2000. *Chinese Journa of Tropical Geography, 38*(6), 799–809.
Xie, Y., & Weng, Q. (2016). Updating urban extents with nighttime light imagery by using an object-based thresholding method. *Remote Sensing of Environment, 187*, 1–13. https://doi.org/10.1016/j.rse.2016.10.002.
Yang, Y., He, C., Zhang, Q., Han, L., & Du, S. (2013). Timely and accurate national-scale mapping of urban land in China using Defense Meteorological Satellite Program's Operational Linescan System nighttime stable light data. *Journal of Applied Remote Sensing, 7*, 73535. https://doi.org/10.1117/1.JRS.7.073535.
Yi, K., Zeng, Y., & Wu, B. (2016). Mapping and evaluation the process, pattern and potential of urban growth in China. *Applied Geography, 71*, 44–55. https://doi.org/10.1016/j.apgeog.2016.04.011.
Zhang, X., Xiao, P., Feng, X., & Yuan, M. (2017). Separate segmentation of multi-temporal high-resolution remote sensing images for object-based change detection in urban area. *Remote Sensing of Environment, 201*, 243–255. https://doi.org/10.1016/j.rse.2017.09.022.
Zhao, M., Zhou, Y., Li, X., Cao, W., He, C., Yu, B., ... Zhou, C. (2019). Applications of satellite remote sensing of nighttime light observations: Advances, challenges, and perspectives. *Remote Sensing, 11*(17), 1971. https://doi.org/10.3390/rs11171971.
Zhou, Y., Li, X., Asrar, G. R., Smith, S. J., & Imhoff, M. (2018). A global record of annual urban dynamics (1992–2013) from nighttime lights. *Remote Sensing of Environment, 219*, 206–220. https://doi.org/10.1016/j.rse.2018.10.015.
Zhou, Y., Smith, S. J., Elvidge, C. D., Zhao, K., Thomson, A., & Imhoff, M. (2014). A cluster-based method to map urban area from DMSP/OLS nightlights. *Remote Sensing of Environment, 147*, 173–185. https://doi.org/10.1016/j.rse.2014.03.004.
Zhou, Y., Smith, S. J., Zhao, K., Imhoff, M., Thomson, A., Bond-Lamberty, B., ... Elvidge, C. D. (2015). A global map of urban extent from nightlights. *Environmental Research Letters, 10*, 54011. https://doi.org/10.1088/1748-9326/10/5/054011.
Zhou, W., Troy, A., & Grove, M. (2008). Object-based Land Cover Classification and Change Analysis in the Baltimore Metropolitan Area Using Multitemporal High Resolution Remote Sensing Data. *Sensors, 8*, 1613–1636. https://doi.org/10.3390/s8031613.
Zou, Y., Peng, H., Liu, G., Yang, K., Xie, Y., & Weng, Q. (2017). Monitoring urban clusters expansion in the middle reaches of the Yangtze River, China, using time-series nighttime light images. *Remote Sensing, 9*(10), 1007. https://doi.org/10.3390/rs9101007.